Table 1. Rat biochemical and metabolic parameters: AGE injection[a]

Parameter	Control	AGE-RSA	AGE-RSA+ALA	RSA
Plasma glucose (mmol/L)	7.4 ± 0.2	7.4 ± 0.2	7.6 ± 0.2	7.9 ± 0.3
GHb (%)	4.1 ± 0.2	3.9 ± 0.2	3.6 ± 0.2	4.1 ± 0.5
Kidney wt:body wt ($\times 10^{-3}$)	5.1 ± 0.1	5.4 ± 0.1	5.5 ± 0.1	5.4 ± 0.1
GFR (ml/min)	4.3 ± 0.1	4.4 ± 0.2	4.1 ± 0.2	4.3 ± 0.3
Systolic BP (mmHg)	114 ± 2	118 ± 2	123 ± 3[b]	121 ± 2
AER (mg/24 h)	1.2 ± 0.8	1.2 ± 0.2	1.3 ± 0.2	1.2 ± 0.1

[a]Data are means ± SEM; n = 6 to 10 per group. AER, albumin excretion rate; GHb, glycated hemoglobin.
[b]$P < 0.01$ *versus* control.

were increased in AGE-RSA–injected rats as compared with RSA (densitometric analysis of RAGE protein expression as determined by Western immunoblotting and corrected to β-actin RSA 202.3 ± 5.7 arbitrary units *versus* AGE-RSA 220.1 ± 1.3 arbitrary units; $n = 3$ rats per group; $P < 0.05$). The cytosol from the renal cortex of AGE-RSA–injected rats also had markedly increased H_2O_2 generation, which was normalized with concomitant ALA therapy (Figure 1C). The RSA vehicle also modestly increased cytosolic H_2O_2 production, although this was significantly lower when compared with AGE-RSA–injected rodents (Figure 1C).

To verify the combined effects of AGE-RAGE interactions on renal H_2O_2 production, we treated RAGE adenoviral vector (Ad-RAGE)-infected cells with AGE-BSA (Ad-RAGE+AGEs) or BSA (Ad-RAGE+BSA). Cytosolic H_2O_2 production was unchanged with Ad-RAGE transfection alone (Figure 1D, Ad-RAGE) or BSA but was significantly increased by more than two-fold with addition of ligand (Ad-RAGE+AGEs), clearly indicating that the AGE-RAGE interaction was required for increased cytosolic H_2O_2 generation in mesangial cells.

AGE-Induced Cytosolic H_2O_2 Liberation Induces mPT and Disrupts Mitochondrial Membrane Potential

Exposure of renal mitochondria to H_2O_2 led to a sequential decrease in absorbance at 540 nm, reflecting induction of mPT (Figure 2A). This decrease in absorbance was inhibited by cyclosporin A (CsA), a classically described agent known to inhibit mPT.[20–22] In addition, an acute AGE-BSA treatment of mesangial cells infected with the RAGE adenovirus led to the liberation of cytosolic H_2O_2 (Figure 2B).

To assess AGE-induced mPT more directly, we treated primary rat mesangial cells with AGE-BSA or BSA for 30 min and cells loaded with calcein-AM with or without cobalt chloride. Mesangial cells that were exposed to AGE-BSA had a significant decrease in calcein fluorescence, indicative of mPT, when compared with cells treated with BSA (Figure 2C). The AGE-mediated decrease in calcein fluorescence was prevented by co-incubation with CsA, confirming the process of mPT. In addition, pretreatment with PEG-catalase (PEG-CAT), a cell-permeable form of catalase, prevented the AGE-BSA–induced mPT (Figure 2C), implicating intracellular H_2O_2 in the process.

To explore further AGE-RAGE–induced mitochondrial dysfunction, we used flow cytometric analysis of cells loaded with the potentiometric dye JC-1 to assess changes in mitochondrial membrane potential ($\Delta\psi_m$). Primary rat mesangial cells were exposed to the uncoupler CCCP as a positive control, which demonstrated a significant loss in red fluorescence in the third (10^3) and fourth (10^4) log, resulting in a leftward shift (Figure 2D, top right), compared with the control empty vector (Figure 2D, top left). This finding is consistent with a decrease in $\Delta\psi_m$ (*i.e.*, depolarization of the inner mitochondrial membrane).[23] Mesangial cells overexpressing RAGE *via* infection with the human full-length Ad-RAGE had a modest but NS loss in red fluorescence compared with the empty vector (Figure 2D, middle left). After addition of the AGE ligand, this leftward shift became more pronounced (Figure 2D, middle right). This was not seen with BSA treatment (Figure 2D, bottom left). In addition, pretreatment with PEG-CAT prevented the AGE-BSA–induced shift (Figure 2D, bottom right). Data from four independent experiments are collated in Figure 2E. Taken together, these data clearly demonstrate AGE-RAGE–induced disruption of $\Delta\psi_m$ and enhanced susceptibility to mPT.

AGE-RAGE Interaction Disrupts the Mitochondrial Respiratory Chain in Normoglycemia, but Hyperglycemia Is Essential for Superoxide Overproduction

To evaluate further whether AGE-induced cytosolic oxidative stress and subsequent mPT could be associated with or could influence changes in the activity of the respiratory chain, we investigated the enzyme complexes I through IV. Initially we identified in an advanced model of diabetes (streptozotocin [STZ]-induced diabetes in Sprague-Dawley rats with no insulin treatment) that complex I activity is selectively decreased by 50% in renal glomeruli compared with control rats (50 ± 10% of control; $n = 6$ rats per group; $P < 0.001$), whereas the remaining OXPHOS complexes were unchanged (complex II 110 ± 8, complexes II+III 105 ± 6, complex III 145 ± 30, and complex IV 125 ± 30% of control; $n = 6$ rats per group). In addition, another previous study[9] would have shown this pattern of electron transport complexes in long-term diabetes if it had corrected for the marker of mitochondrial activity, citrate synthase, which is elevated in renal mitochondria from diabetic rats (control 76.9 ± 9.1 *versus* diabetic 114.5 ± 4.0 nmol/min per mg; $n = 5$ rats per group; $P < 0.01$). On the basis of these results, we focused on complex I alone as a target of dysfunction in our rodent models.

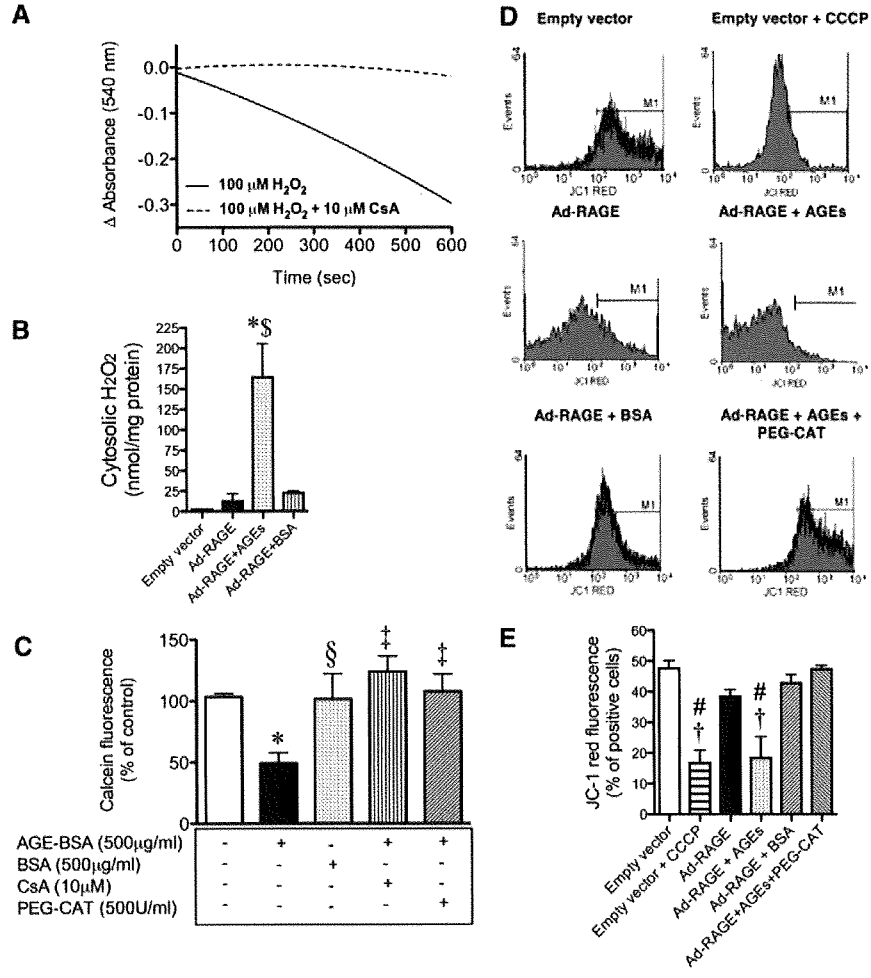

Figure 2. AGE-induced cytosolic H_2O_2 liberation induces mPT and disrupts mitochondrial membrane potential. (A) H_2O_2-induced swelling of renal cortical mitochondria. Mitochondria were incubated with 100 μM H_2O_2 with or without 10 μM CsA for 10 min, and mPT was followed by a decrease in absorbance at 540 nm. Trace is representative of three independent experiments. (B) Cytosolic H_2O_2 in primary rat mesangial cells infected with the human FL Ad-RAGE or the control empty vector for 72 h. At 24 h after infection, either AGE-BSA (500 μg/ml) or BSA (500 μg/ml) was added for 15 min. Samples shown are representative of three independent experiments. Bars represent means ± SEM, $n = 3$. (C) Primary rat mesangial cells were treated with 500 μg/ml AGE-BSA or 500 μg/ml BSA for 30 min, and cells were loaded with 2 μM calcein-AM with or without 1 mM cobalt chloride for 30 min at 37°C to assess mPT. A decrease in fluorescence indicates opening of the mitochondrial transition pore. Appropriate cells were pretreated with either 10 μM CsA or 500 U/ml PEG-CAT for 30 min at 37°C. Data are representative of three independent experiments. Bars represent means ± SEM, $n = 3$. (D) FACS analysis of mitochondrial membrane potential ($\Delta\psi_m$) in primary rat mesangial cells infected with the human FL Ad-RAGE or the control empty vector for 72 h. At 24 h after infection, either AGE-BSA (100 μg/ml) or BSA (100 μg/ml) was added to one group. Cells were stained with 2 μM JC-1 and analyzed on a flow cytometer. CCCP, a mitochondrial membrane potential disrupter, was used as a positive control, and PEG-CAT (500U/ml) was used to detoxify intracellular H_2O_2. (E) JC-1 red fluorescence quantification. Data are representative of four independent experiments. *$P < 0.05$ *versus* control or empty vector; †$P < 0.01$ *versus* Ad-RAGE; ‡$P < 0.01$ *versus* AGE-BSA; §$P < 0.05$ *versus* AGE-BSA; #$P < 0.001$ *versus* empty vector; $$P < 0.001$ *versus* Ad-RAGE.

In vivo, long-term injection of AGE-RSA (16 wk) induced a 50% suppression of complex I activity in renal glomeruli as compared with both sham-injected rats (control) and rats injected with RSA (Figure 3A). Of note, modest inhibition of complex I activity was also seen in rodents injected long-term with RSA alone. Generation of mitochondrial superoxide was unchanged by long-term AGE-RSA injection in the absence of hyperglycemia (Figure 3B).

Consistent with previous studies, diabetic rats had significantly elevated plasma glucose and glycated hemoglobin and an increase in kidney-to-body weight ratio compared with control rats (Table 2). By 16 wk of diabetes, significant elevations in systolic BP and albumin excretion rate were evident, which were further increased by 32 wk of diabetes (Table 2). Induction of RAGE gene expression was seen at both 16 and 32 wk of diabetes (see Supplemental Appendix; Figure 2). As observed in the AGE injection model, there was increased cytosolic H_2O_2 at weeks 16 and 32 of diabetes (see Supplemental Appendix; Figure 3).

Renal glomerular complex I activity was unchanged after 16 wk of diabetes; however, by 32 wk, there was a significant decline in glomerular complex I activity of 30% compared with control (Figure 3C). In contrast to results for AGE-injected rodents, by 32 wk of disease, complex I deficiency in diabetic glomeruli was accompanied by a significant overproduction of mitochondrial superoxide (Figure 3D). Strikingly, renal mitochondria from diabetic rats treated with the cytosolic NADPH oxidase inhibitor, APO, or ALA, the inhibitor of AGE accumulation had less superoxide production with levels similar to those seen in healthy rats (Figure 3D). Furthermore, ALA restored glomerular complex I activity to control levels (Figure 3C). The superoxide overproduction was observed in the context of decreased activity of MnSOD in renal mitochondria from diabetic rats (see Supplemental Appendix; Figure 4).

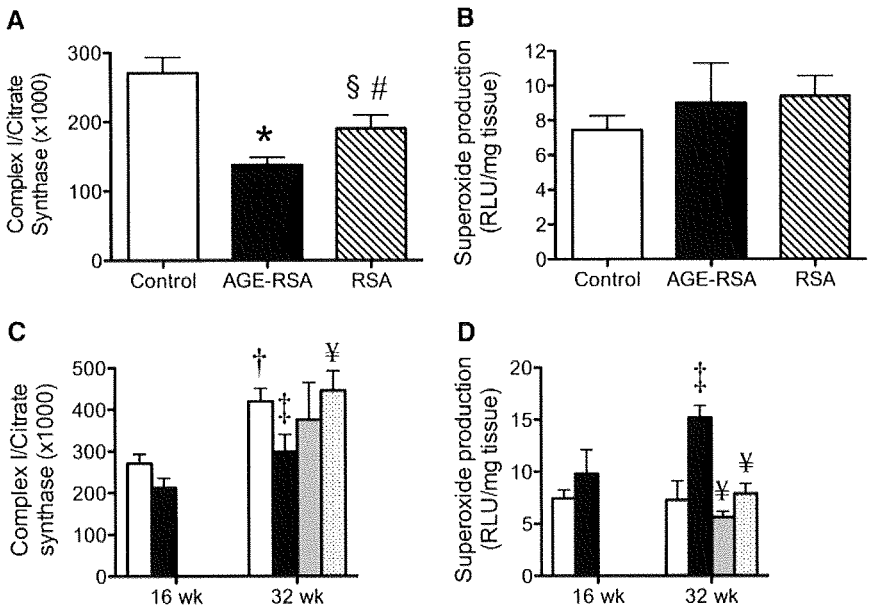

Figure 3. The AGE-RAGE interaction disrupts the mitochondrial respiratory chain in normoglycemia, but hyperglycemia is essential for superoxide overproduction. (A and B) Representative of renal glomeruli or renal cortex of AGE-RSA or RSA-injected (20 mg/kg per d) rats for 16 wk (n = 6 to 10 rats per group). (A) Glomerular complex I (NADH: ubiquinone oxidoreductase) activity expressed relative to citrate synthase activity. (B) NADH-driven (mitochondrial) superoxide production was measured by lucigenin-enhanced chemiluminescence. (C and D) Representative of renal glomeruli or renal cortex of diabetic rats (■) or control rats (□) followed for 16 or 32 wk. A subset of diabetic rats received the NADPH oxidase inhibitor APO (▨; 15 mg/kg per d) or the AGE inhibitor ALA chloride (⊡; 10 mg/kg per d) from week 16 to 32. (C) Glomerular complex I activity expressed relative to citrate synthase activity. (D) NADH-driven (mitochondrial) superoxide production. Bars represent means ± SEM, n = 6 to 10 rats per group. *$P < 0.001$ *versus* control; †$P < 0.001$ *versus* 16-wk control; ‡$P < 0.05$ *versus* 32-wk control; §$P < 0.05$ *versus* AGE-RSA; #$P < 0.05$ *versus* control; ¥$P < 0.05$ *versus* 32-wk diabetes.

Table 2. Rat biochemical and metabolic parameters: STZ-induced diabetes[a]

Parameter	16 Wk		32 Wk	
	Control	Diabetes	Control	Diabetes
Plasma glucose (mmol/L)	7.4 ± 0.2	34.5 ± 0.5[b]	6.9 ± 0.2	33.2 ± 0.7[b]
GHb (%)	4.1 ± 0.2	17.3 ± 1.0[b]	5.5 ± 0.2	18.3 ± 0.7[b]
Kidney wt:body wt ($\times 10^{-3}$)	5.1 ± 0.1	10.9 ± 0.6[b]	5.3 ± 0.2	11.3 ± 0.4[b]
GFR (ml/min)	4.3 ± 0.1	4.5 ± 0.3	4.8 ± 0.2	4.6 ± 0.1
Systolic BP (mmHg)	106 ± 2	140 ± 4[c]	114 ± 2	134 ± 3[c]
AER (mg/24 h)	1.2 ± 0.8	29.9 ± 7.5[b]	5.6 ± 1.9	48.9 ± 16.0[b]

[a]Data are means ± SEM; n = 6 to 10 per group.
[b]$P < 0.001$ *versus* respective control.
[c]$P < 0.05$ *versus* respective control.

AGE-RAGE Interaction and High Glucose Are Critical for Superoxide Overproduction, Facilitated by Induction of mPT

Mesangial cells overexpressing RAGE and exposed to AGEs (Ad-RAGE+AGE) had decreased complex I activity in both normal- and high-glucose environments (Figure 4A). There was, however, no increase in mitochondrial superoxide production in Ad-RAGE–infected cells exposed to normal glucose and AGEs (Figure 4B). Although no excess superoxide generation was evident in Ad-RAGE–infected cells incubated in high glucose in the absence of AGE-BSA (Figure 4B), there was a three-fold increase upon exposure to both high glucose and AGEs (Figure 4B). Similarly, increased cytochrome C release from the mitochondria was evident only in Ad-RAGE–infected cells incubated with both high glucose and AGEs (Figure 4C). In addition, caspase 3 was activated in Ad-RAGE–infected mesangial cells exposed to AGEs and high glucose, and this increase in apoptosis was inhibited by the mPT inhibitor adenosine 5′diphosphate (ADP; see Supplemental Appendix; Figure 5).

To confirm that AGE-RAGE interactions caused excess mitochondrial superoxide generation *via* mPT in high-glucose environments, we incubated Ad-RAGE–infected primary mesangial cells with various mPT inhibitors in the presence and absence of AGE-BSA. Indeed, significant inhibition of AGE-RAGE–induced mitochondrial superoxide generation was observed with the addition of two disparate inhibitors of mPT, CsA and ADP (Figure 4D).

Mitochondrial superoxide generation was also elevated in renal cortices from wild-type (WT) mice after 24 wk of diabetes when compared with control WT mice (Figure 4E). Conversely, no increase in the production of mitochondrial superoxide was seen in renal cortices from diabetic RAGE−/− mice. This lack of mitochondrial ROS production in diabetic RAGE−/− mice occurred in the context of reduced albuminuria in these mice when compared with WT diabetic mice (WT control 155 ± 41, WT diabetic 410 ± 75 μg/24 h [$P < 0.05$ WT control *versus* WT diabetic]; RAGE−/− control 142 ± 51; RAGE−/− diabetic 158 ± 50 μg/24 h [$P < 0.05$ WT diabetic *versus* RAGE−/− diabetic]). Furthermore, analysis of apopto-

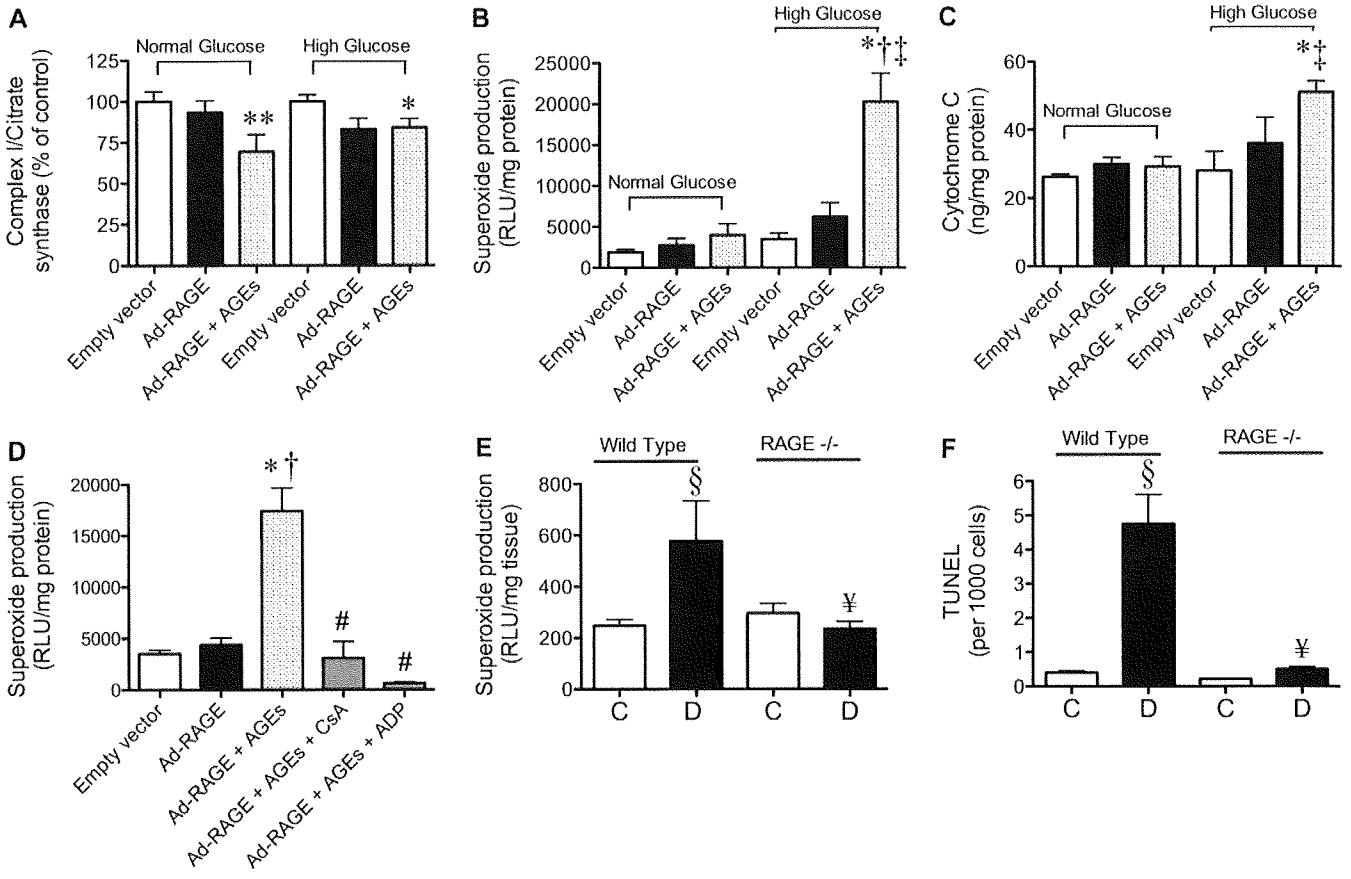

Figure 4. The AGE-RAGE interaction and high glucose amplify renal mitochondrial superoxide generation, facilitated by induction of mPT. (A through C) Representative of primary rat mesangial cells cultured in normal glucose (5.5 mM) or high glucose (25 mM) and infected with the human FL Ad-RAGE or the control empty vector for 72 h. At 24 h after infection, AGE-BSA (100 μg/ml) was added to one group (Ad-RAGE+AGEs). (A) Mitochondrial complex I activity expressed relative to citrate synthase activity. (B) Mitochondrial NADH-driven superoxide generation was measured by lucigenin-enhanced chemiluminescence. (C) Cytochrome C release from mitochondria determined by ELISA. Inhibitors of mPT, CsA (10 μM) and ADP (100 μM), were also given to some groups 24 h after infection in the presence of 100 μg/ml AGE-BSA. (D) Mitochondrial NADH-driven superoxide generation from cells treated with high glucose (25 mM) after inhibition of mPT. Bars represent means ± SEM, $n = 3$ independent cell culture experiments. (E and F) Representative of renal cortical samples from control (□) and diabetic (■) WT (C57BL/6J) and RAGE−/− mice at week 24 after the induction of STZ diabetes ($n = 10$ mice per group). (E) NADH-driven superoxide production. (F) Terminal deoxynucleotidyl transferase–mediated digoxigenin-deoxyuridine nick-end labeling in renal cortices expressed per 1000 cells counted. *$P < 0.001$ *versus* control empty vector high glucose; **$P < 0.05$ *versus* control empty vector normal glucose; †$P < 0.01$ *versus* Ad-RAGE in high glucose; ‡$P < 0.05$ *versus* Ad-RAGE+AGEs in normal glucose; §$P < 0.05$ *versus* wild type control 24W; #$P < 0.001$ *versus* Ad-RAGE+AGEs; ¥$P < 0.05$ *versus* WT diabetic 24 wk.

tic cells in renal cortices demonstrated a diabetes-specific increase in WT mice when compared with control WT mice (Figure 4F). Diabetes, however, was not associated with an increase in apoptosis in renal cortices from diabetic RAGE−/− mice. In addition to this, cytosolic ROS production was blocked in diabetic RAGE−/− mice compared with WT diabetic mice (Supplemental Figure 6).

OXPHOS Substrate Availability Is Crucial for Superoxide-Induced Renal Dysfunction in Diabetes

Finally, we examined the substrate availability of the pyridine nucleotide NADH, which is essential for complex I function *in vivo*. Mesangial cells infected with Ad-RAGE in high-glucose environments had significant increases in mitochondrial NADH content that were not seen in Ad-RAGE cells incubated in normal-glucose conditions (Figure 5A). Indeed, in normal glucose, Ad-RAGE–infected cells had a depletion of NADH content within the mitochondria when compared with the empty vector alone. In addition, in rat renal cortical mitochondria, NADH content was depleted 50% after long-term AGE injection in healthy normoglycemic rodents when compared with control and RSA-treated rats (Figure 5B). This depletion was not *via* an inhibition of glycolysis, because cytosolic lactate concentration was similar between groups (data not shown). In contrast, there was no depletion of NADH content in renal mitochondria from

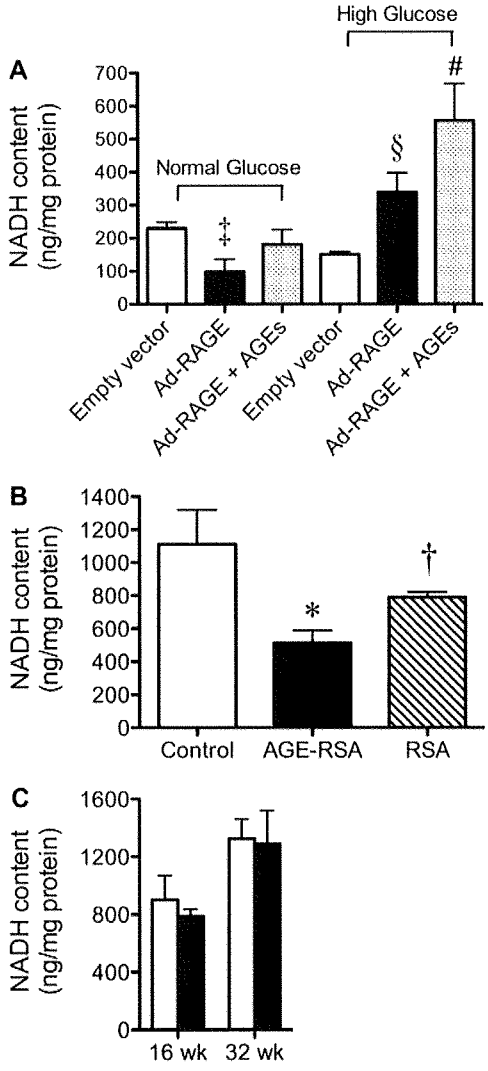

Figure 5. OXPHOS substrate availability is crucial for superoxide-induced renal dysfunction in diabetes. (A) Primary mesangial cells cultured in high glucose (25 mM) were infected with the human FL Ad-RAGE or the control empty vector for 72 h. At 24 h after infection, AGE-BSA (100 μg/ml) was added to one group (Ad-RAGE+AGEs). NADH content of isolated mitochondria. Mitochondria were isolated from the renal cortex of STZ-induced diabetic rats followed for 16 or 32 wk and from rats injected with AGE-RSA for 16 wk. (B and C) NADH content was determined in mitochondria from AGE-injected rats (B) and mitochondria from STZ-induced diabetic rats (C). □, control; ■, diabetes group. Bars represent means ± SEM, $n = 6$ to 10 rats per group. *$P < 0.05$ *versus* control; †$P < 0.05$ *versus* AGE-RSA; ‡$P < 0.05$ *versus* empty vector cultured in normal glucose; §$P < 0.05$ *versus* Ad-RAGE cultured in normal glucose; #$P < 0.05$ *versus* Ad-RAGE+AGEs cultured in normal glucose.

diabetic rodents at week 16 or 32 compared with nondiabetic rats (Figure 5C), consistent with the presence of sufficient substrate levels to drive complex I and thereby generate superoxide radicals.

DISCUSSION

This series of *in vitro* and *in vivo* studies demonstrated that both impairment of function and adequate substrate availability for the respiratory chain are critical for the subsequent amplification of mitochondrial superoxide in the kidney in diabetes. We demonstrated that the interaction between AGEs and RAGE liberates cytosolic ROS, which leads to the induction of mPT, a phenomenon that proceeded even in the absence of hyperglycemia. Opening of the mitochondrial transition pore and resultant swelling seemed to induce a decrease in the activity of complex I of the respiratory chain. Perhaps the most striking finding in our study was that once electron leakage from the respiratory chain occurred, which was not glucose dependent, generation of excess mitochondrial superoxide was seen only in the setting of high glucose. Our studies support and extend the hypothesis that overproduction of mitochondrial ROS is a key event in activating pathways implicated in the development of the complications of diabetes.[2] Furthermore, we specifically highlighted the importance of the cytosolic compartment in enhancing and indeed facilitating mitochondrial generation of ROS. This indicates that cytosolic events, as a result of the AGE-RAGE interaction, play a key role in amplifying mitochondrial ROS generation in the kidney.

Activation of RAGE is known to induce NADPH oxidase and cellular ROS production in endothelial cells *in vitro*.[24] In the diabetic context, this study extends these findings by demonstrating that interactions between AGEs and RAGE stimulate the cytosolic production of ROS within the renal cortex, and this is inhibited by the NADPH oxidase inhibitor APO. It was also of interest that cellular RAGE overexpression alone in the absence of elevated AGEs could not increase cytosolic H_2O_2 production that was seen with concomitant AGE exposure. This suggests that ligand binding is an important event in AGE-RAGE–mediated production of cytosolic ROS. Furthermore, our own recent study demonstrated the utility of APO as a therapy for diabetic renal disease, confirming *in vivo* that AGE-RAGE ligation can activate NADPH oxidase.[25]

ROS in particular, the more stable H_2O_2, are widely known inducers of mPT in tissues other than the kidney.[26,27] Hence, we confirmed these findings in renal mitochondria by demonstrating that addition of exogenous H_2O_2 induces mPT. Furthermore, AGE-BSA exposure caused mPT in excess of that seen in untreated mesangial cells, in addition to disrupting the mitochondrial membrane potential, both of which were reversed by detoxifying intracellular H_2O_2 with catalase. Importantly, these changes were independent of ambient glucose concentrations. Thus, it was proposed that AGE-induced intracellular H_2O_2 formation played a significant role in enhancing susceptibility to the mPT; however, cytochrome C release from mitochondria, indicative of induction of apoptosis,[28] was observed only in groups cultured in high-glucose environments. Furthermore, diabetic RAGE−/− mice were protected from renal cellular apoptosis when compared with WT diabetic mice. Indeed, there is increased apoptosis in mesangial

cells isolated from STZ-induced diabetic rats,[29] and AGE-RAGE interactions were postulated to contribute to podocyte apoptosis.[30] Furthermore, other groups demonstrated protection against the induction of diabetic nephropathy by inhibition of cellular apoptosis,[31,32] which is consistent with the improved renal function in the context of less renal apoptosis seen in RAGE−/− mice from this study.

Studies have suggested that patients with genetic mutations leading to a dysfunctional mitochondrial respiratory chain can present with renal disease as their primary pathology.[7,8] One such disorder, Friedreich ataxia, has specific electron leakage at complexes I and III leading to excessive generation of superoxide.[6] In our study, we showed that within diabetic glomeruli, there seems to be a specific defect in complex I rather than other complexes of the respiratory chain. In other contexts, opening of the mPT pore induces electron leakage, leading to increased mitochondrial ROS production at the level of complex I.[11] In that study, mitochondrial ROS production was observed only in the presence of a continued supply of the complex I substrate NADH to the respiratory chain, because mPT led to depletion of NADH through diffusion of pyridine nucleotides out of the mitochondria. Hence, these investigators postulated that mPT induces a decline in the activity of complex I, which dramatically increases ROS production as long as electrons are provided to complex I.[11] In addition, a recent study elegantly demonstrated that transient opening of the mPT pore stimulated spontaneous bursts of superoxide generation by the mitochondrial respiratory chain.[33] Indeed, our own studies in RAGE overexpressing cells exposed to AGE-BSA demonstrated an abrogation of excess mitochondrial superoxide production in the presence of inhibitors of mPT. Furthermore, although a decline in complex I activity could be seen in various settings of normoglycemia in this series of studies, there was no increase in superoxide generation as a result of the depletion of mitochondrial NADH. Indeed, our AGE-injected nondiabetic rats had little evidence of progressive nephropathy at the time point studied. In our diabetic rats, however, the mitochondrial NADH pool seemed sufficient to supply reducing equivalents to complex I, thereby sustaining mitochondrial superoxide production. Furthermore, this mitochondrial superoxide overproduction was exacerbated by decreased activity of mitochondrial MnSOD.

A previous study found that mitochondria from the renal cortex of rats with diabetes exhibited a diminution of OXPHOS *via* decreased complex III activity and increased superoxide formation.[9] In that particular study, however, the measurement of OXPHOS enzymes was not normalized to citrate synthase activity, a procedure considered critical to correct for changes in total mitochondrial number between kidneys from control and diabetic rats; therefore, in that study, one cannot exclude that the decreased OXPHOS reported is in fact due to changes in other subunits of the respiratory chain. Nevertheless, the observation in that study of increased renal mitochondrial superoxide production in STZ-induced diabetes is consistent with the work described in this study. This is further supported by our studies, which included evaluation of the role of RAGE *per se*. Specifically, the diabetes-induced increases in renal mitochondrial superoxide generation were observed in WT mice but not in kidneys from diabetic RAGE−/− mice.

In conclusion, our data indicate that chronic hyperglycemia, leading to enhanced NADH-derived electron delivery to complex I, is required in conjunction with AGE-RAGE–induced cytosolic H_2O_2 activation of mPT to generate excessive mitochondrial superoxide (Figure 6). This indicates not only does the cytosol act in concert with the mitochondria to generate cellular ROS but also that cytosolic ROS generation may cause or amplify some of the specific mitochondrial defects observed in diabetes. These defects include complex I deficiency, enhanced susceptibility to mPT, and ultimately overproduction of superoxide, which is considered to play a central role in inducing diabetic end-organ injury. The observations presented here suggest that pharmacologic inhibition of cytosolic ROS production may be an appropriate strategy to reduce excessive mitochondrial superoxide production in diabetic complications. In addition, it is postulated that therapies that target complex I may restore mitochondrial integrity and potentially confer a degree of renoprotection in diabetes.

CONCISE METHODS

An expanded version of the Concise Methods section is available in the Supplemental Appendix.

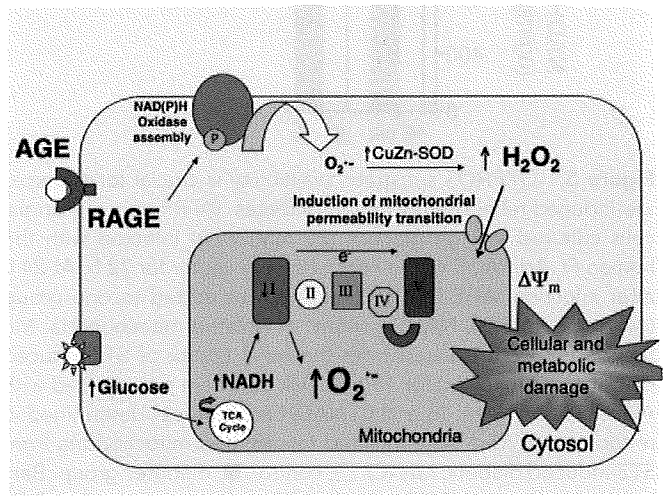

Figure 6. Schematic representation of the interplay between AGE and RAGE and high glucose in promoting mitochondrial superoxide production in the diabetic kidney. AGEs binding to RAGE induce cytosolic H_2O_2 production. Cytosolic H_2O_2 facilitates induction of mPT, promoting a deficiency in complex I of the mitochondrial respiratory chain. Hyperglycemia provides increased mitochondrial NADH availability for OXPHOS, which, when coupled with a deficient complex I activity, amplifies mitochondrial superoxide generation. Both the AGE-RAGE interaction and hyperglycemia synergistically coordinate overproduction of mitochondrial superoxide and promote diabetic kidney disease.

In Vivo Rodent Studies

All animal experiments were performed in accordance with the Alfred Medical Research and Education Precinct Animal Ethics committee.

STZ-Induced Diabetes.
Experimental diabetes was induced in male Sprague-Dawley rats[34] or WT (C57BL/6J; Jackson Laboratories, Bar Harbor, ME) and RAGE-deficient mice (RAGE−/−)[35,36] with STZ as described previously[37] with control rodents followed concurrently. Diabetic and control animals were randomized ($n = 10$ per group) and followed for 16 or 32 wk for rats or 24 wk for mice. A subset of diabetic rats ($n = 10$) received either the NADPH oxidase inhibitor APO (15 mg/kg per d, oral gavage) or the AGE inhibitor ALA chloride [4,5-dimethyl-3-(2-oxo2-phenylethyl)-thiazolium chloride, a gift from Synvista, Ramsey, NJ; 10 mg/kg per d, oral gavage] from weeks 16 to 32. Two units of Ultralente insulin (Novo Nordisk, Bagsværd, Denmark) were administered daily to diabetic rats to prevent ketoacidosis and improve survival.

Exogenous AGE Administration.
Endotoxin-free AGE-RSA was prepared as described previously.[19] Exogenous AGE-RSA was administered daily to healthy 8-wk-old Sprague-Dawley rats ($n = 10$ per group); AGE-RSA (20 mg/kg per d, intraperitoneally), RSA (20 mg/kg per d, intraperitoneally), or saline (controls) for 16 wk.[38] An additional AGE-RSA subgroup ($n = 10$) was randomized to receive treatment with the AGE inhibitor ALA chloride (10 mg/kg per d, oral gavage) for the duration of the study. Sixteen weeks was chosen on the basis of previous studies that documented the time course of renal disease in this rat model.[38]

Construction and Generation of Recombinant Adenovirus Vectors.
A recombinant adenovirus encoding human RAGE was constructed and generated. Full-length human RAGE cDNA (gift of Prof. H. Yamamoto[39]) was inserted into the shuttle plasmid pAdTrack-CMV containing a GFP reporter and was then subcloned into the adenoviral backbone plasmid AdEasy-1 (Ad-RAGE). Human embryonic kidney 293 cells were then infected to package the virus using lipofectamine 2000 reagent (Invitrogen, Melbourne, Australia). The pAdTrack-CMV shuttle vector without the gene of interest was used as a control (empty vector). RAGE expression was verified using Western immunoblotting (see Supplemental Appendix, Figure 1).

Adenovirus-Mediated RAGE Gene Transfer In Vitro.
Primary mesangial cells were isolated from rat kidney as described previously.[40] Mesangial cells seeded into 75-cm^2 tissue culture flasks were grown for 3 d to 60% confluence in 5.5 mM D-glucose in DMEM containing 10% FCS; then the medium was replaced with DMEM containing either 5.5 or 25.0 mM D-glucose and the purified Ad-RAGE vector or empty vector (2.85×10^8 optical particle units). After 24 h, 100 μg/ml AGE-BSA or 100 μg/ml BSA was added, and cells were cultured for an additional 2 d. In some studies, inhibitors of mitochondrial pore transition, ADP (100 μM) and CsA (10 μM), or the antioxidant PEG-catalase (500 U/ml), were concomitantly administered with AGE-BSA. Transfection efficiency was 80 to 90% on the basis of GFP fluorescence.

Mitochondrial Superoxide Production.
Superoxide production in renal cortex was determined by lucigenin-enhanced chemiluminescence as described previously.[34] Superoxide production in freshly isolated mitochondria from primary mesangial cells was measured as described previously.[1]

H_2O_2 Production.
Please refer to the expanded version of the Methods section of the Supplemental Appendix.

Superoxide Dismutase Activity.
Please refer to the expanded version of the Methods section of the Supplemental Appendix.

Mitochondrial Membrane Potential.
Mitochondrial membrane potential was assessed using the MitoProbe JC-1 assay kit (Molecular Probes, Eugene, Oregon) by flow cytometry, according to the manufacturer's instructions.

OXPHOS Complex Activity.
Isolation of renal glomeruli was performed as described previously.[41] Respiratory chain complexes and citrate synthase were assayed in glomerular supernatants and in mesangial cell mitochondrial preparations as described previously for other tissues.[42] For accounting for variations in mitochondrial number between samples, complex activity was expressed relative to citrate synthase, which is much more resistant to oxidative inactivation than the respiratory chain complexes.[43]

Apoptosis.
Please refer to the expanded version of the Methods section of the Supplemental Appendix.

Mitochondrial Permeability Transition.
Please refer to the expanded version of the Methods section of the Supplemental Appendix.

Mitochondrial NADH Content.
Mitochondria (50-μl suspension) from renal cortex or from primary rat mesangial cells were alkaline treated (50 μl of 1 M NaOH) at 90°C for 5 min to destroy the oxidized NAD^+ isoform. Samples were quenched on ice and neutralized, and NADH content was measured using a modification of the method originally described by Nisselbaum and Green.[44]

Real-Time Reverse Transcription–PCR.
Please refer to the expanded version of the Methods section of the Supplemental Appendix.

Statistical Analysis

All statistical computations were performed using GraphPad Prism 4.0a for Mac OS X (GraphPad Software, San Diego, CA). Values of experimental groups are given as mean, with bars showing the SEM, unless otherwise stated. One-way ANOVA with Tukey posttest analysis or two-way ANOVA with Bonferroni posttest analysis was used to

determine statistical significance. When appropriate, two-tailed *t* test were performed. $P < 0.05$ was considered to be statistically significant.

ACKNOWLEDGMENTS

This research was funded by a Juvenile Diabetes Research Foundation Center Grant (J.M.F., M.E.C., A.B., P.P.N., and M.B.), a National Health and Medical Research Council of Australia (NHMRC) Project Grant (J.F., D.T., and M.E.C.), and a Diabetes Australia Research Trust Millennium Grant (J.M.F.). J.M.F. is a recipient of a Juvenile Diabetes Research Foundation Career Development Award. D.R.T. holds an NHMRC Principal Research Fellowship, and M.E.C. holds an NHMRC Senior Principal Research Fellowship. In addition, this work was in part supported by a grant from the Deutsche Forschungsgemeinschaft (SFB405 to P.P.N.).

We thank Susan Thorpe for the analysis of the AGE-BSA and AGE-RSA for AGE content and acknowledge the technical assistance of Maryann Arnstein, Gavin Langmaid, Sandra Miljavec, Felicia Y.T. Yap, Anna Gasser, David C.K. Tong, and Josefa Pete.

DISCLOSURES

None.

REFERENCES

1. Pitkanen S, Robinson BH: Mitochondrial complex I deficiency leads to increased production of superoxide radicals and induction of superoxide dismutase. *J Clin Invest* 98: 345–351, 1996
2. Nishikawa T, Edelstein D, Du XL, Yamagishi S, Matsumura T, Kaneda Y, Yorek MA, Beebe D, Oates PJ, Hammes HP, Giardino I, Brownlee M: Normalizing mitochondrial superoxide production blocks three pathways of hyperglycaemic damage. *Nature* 404: 787–790, 2000
3. Baynes JW, Thorpe SR: Role of oxidative stress in diabetic complications: A new perspective on an old paradigm. *Diabetes* 48: 1–9, 1999
4. Koopman WJ, Verkaart S, Visch HJ, van der Westhuizen FH, Murphy MP, van den Heuvel LW, Smeitink JA, Willems PH: Inhibition of complex I of the electron transport chain causes O2−.-mediated mitochondrial outgrowth. *Am J Physiol Cell Physiol* 288: C1440–C1450, 2005
5. Beyer RE: An analysis of the role of coenzyme Q in free radical generation and as an antioxidant. *Biochem Cell Biol* 70: 390–403, 1992
6. Rotig A, de Lonlay P, Chretien D, Foury F, Koenig M, Sidi D, Munnich A, Rustin P: Aconitase and mitochondrial iron-sulphur protein deficiency in Friedreich ataxia. *Nat Genet* 17: 215–217, 1997
7. Martin-Hernandez E, Garcia-Silva MT, Vara J, Campos Y, Cabello A, Muley R, Del Hoyo P, Martín MA, Arenas J: Renal pathology in children with mitochondrial diseases. *Pediatr Nephrol* 20: 1299–1305, 2005
8. Singh PJ, Santella RN, Zawada ET: Mitochondrial genome mutations and kidney disease. *Am J Kidney Dis* 28: 140–146, 1996
9. Rosca MG, Mustata TG, Kinter MT, Ozdemir AM, Kern TS, Szweda LI, Brownlee M, Monnier VM, Weiss MF: Glycation of mitochondrial proteins from diabetic rat kidney is associated with excess superoxide formation. *Am J Physiol Renal Physiol* 289: F420–F430, 2005
10. Oliveira PJ, Esteves TC, Seica R, Moreno AJ, Santos MS: Calcium-dependent mitochondrial permeability transition is augmented in the kidney of Goto-Kakizaki diabetic rat. *Diabetes Metab Res Rev* 20: 131–136, 2004
11. Batandier C, Leverve X, Fontaine E: Opening of the mitochondrial permeability transition pore induces reactive oxygen species production at the level of the respiratory chain complex I. *J Biol Chem* 279: 17197–17204, 2004
12. Kabat A, Ponicke K, Salameh A, Mohr FW, Dhein S: Effect of a beta 2-adrenoceptor stimulation on hyperglycemia-induced endothelial dysfunction. *J Pharmacol Exp Ther* 308: 564–573, 2004
13. Brownlee M: Biochemistry and molecular cell biology of diabetic complications. *Nature* 414: 813–820, 2001
14. Forbes JM, Thallas V, Thomas MC, Founds HW, Burns WC, Jerums G, Cooper ME: The breakdown of preexisting advanced glycation end products is associated with reduced renal fibrosis in experimental diabetes. *FASEB J* 17: 1762–1764, 2003
15. Wendt TM, Tanji N, Guo J, Kislinger TR, Qu W, Lu Y, Bucciarelli LG, Rong LL, Moser B, Markowitz GS, Stein G, Bierhaus A, Liliensiek B, Arnold B, Nawroth PP, Stern DM, D'Agati VD, Schmidt AM: RAGE drives the development of glomerulosclerosis and implicates podocyte activation in the pathogenesis of diabetic nephropathy. *Am J Pathol* 162: 1123–1137, 2003
16. Basta G, Lazzerini G, Del Turco S, Ratto GM, Schmidt AM, De Caterina R: At least 2 distinct pathways generating reactive oxygen species mediate vascular cell adhesion molecule-1 induction by advanced glycation end products. *Arterioscler Thromb Vasc Biol* 25: 1401–1407, 2005
17. Cai W, He JC, Zhu L, Lu C, Vlassara H: Advanced glycation end product (AGE) receptor 1 suppresses cell oxidant stress and activation signaling *via* EGF receptor. *Proc Natl Acad Sci U S A* 103: 13801–13806, 2006
18. Degenhardt TP, Alderson NL, Arrington DD, Beattie RJ, Basgen JM, Steffes MW, Thorpe SR, Baynes JW: Pyridoxamine inhibits early renal disease and dyslipidemia in the streptozotocin-diabetic rat. *Kidney Int* 61: 939–950, 2002
19. Oldfield MD, Bach LA, Forbes JM, Nikolic-Paterson D, McRobert A, Thallas V, Atkins RC, Osicka T, Jerums G, Cooper ME: Advanced glycation end products cause epithelial-myofibroblast transdifferentiation *via* the receptor for advanced glycation end products (RAGE). *J Clin Invest* 108: 1853–1863, 2001
20. Broekemeier KM, Dempsey ME, Pfeiffer DR: Cyclosporin A is a potent inhibitor of the inner membrane permeability transition in liver mitochondria. *J Biol Chem* 264: 7826–7830, 1989
21. Crompton M, Ellinger H, Costi A: Inhibition by cyclosporin A of a Ca2+-dependent pore in heart mitochondria activated by inorganic phosphate and oxidative stress. *Biochem J* 255: 357–360, 1988
22. Fournier N, Ducet G, Crevat A: Action of cyclosporine on mitochondrial calcium fluxes. *J Bioenerg Biomembr* 19: 297–303, 1987
23. Brunt KR, Fenrich KK, Kiani G, Tse MY, Pang SC, Ward CA, Melo LG: Protection of human vascular smooth muscle cells from H2O2-induced apoptosis through functional codependence between HO-1 and AKT. *Arterioscler Thromb Vasc Biol* 26: 2027–2034, 2006
24. Wautier MP, Chappey O, Corda S, Stern DM, Schmidt AM, Wautier JL: Activation of NADPH oxidase by AGE links oxidant stress to altered gene expression *via* RAGE. *Am J Physiol Endocrinol Metab* 280: E685–E694, 2001
25. Thallas-Bonke V, Thorpe SR, Coughlan MT, Fukami K, Yap FY, Sourris KC, Penfold SA, Bach LA, Cooper ME, Forbes JM: Inhibition of NADPH oxidase prevents advanced glycation end product-mediated damage in diabetic nephropathy through a protein kinase C-alpha-dependent pathway. *Diabetes* 57: 460–469, 2008
26. Colell A, Garcia-Ruiz C, Mari M, Fernandez-Checa JC: Mitochondrial permeability transition induced by reactive oxygen species is independent of cholesterol-regulated membrane fluidity. *FEBS Lett* 560: 63–68, 2004
27. Takeyama N, Miki S, Hirakawa A, Tanaka T: Role of the mitochondrial permeability transition and cytochrome C release in hydrogen peroxide-induced apoptosis. *Exp Cell Res* 274: 16–24, 2002

28. Liu X, Kim CN, Yang J, Jemmerson R, Wang X: Induction of apoptotic program in cell-free extracts: Requirement for dATP and cytochrome c. *Cell* 86: 147–157, 1996
29. Weissgarten J, Berman S, Efrati S, Rapoport M, Averbukh Z, Feldman L: Apoptosis and proliferation of cultured mesangial cells isolated from kidneys of rosiglitazone-treated pregnant diabetic rats. *Nephrol Dial Transplant* 21: 1198–1204, 2006
30. Chuang PY, Yu Q, Fang W, Uribarri J, He JC: Advanced glycation endproducts induce podocyte apoptosis by activation of the FOXO4 transcription factor. *Kidney Int* 72: 965–976, 2007
31. Isermann B, Vinnikov IA, Madhusudhan T, Herzog S, Kashif M, Blautzik J, Corat MA, Zeier M, Blessing E, Oh J, Gerlitz B, Berg DT, Grinnell BW, Chavakis T, Esmon CT, Weiler H, Bierhaus A, Nawroth PP: Activated protein C protects against diabetic nephropathy by inhibiting endothelial and podocyte apoptosis. *Nat Med* 13: 1349–1358, 2007
32. Susztak K, Raff AC, Schiffer M, Bottinger EP: Glucose-induced reactive oxygen species cause apoptosis of podocytes and podocyte depletion at the onset of diabetic nephropathy. *Diabetes* 55: 225–233, 2006
33. Wang W, Fang H, Groom L, Cheng A, Zhang W, Liu J, Wang X, Li K, Han P, Zheng M, Yin J, Wang W, Mattson MP, Kao JP, Lakatta EG, Sheu SS, Ouyang K, Chen J, Dirksen RT, Cheng H: Superoxide flashes in single mitochondria. *Cell* 134: 279–290, 2008
34. Coughlan MT, Thallas-Bonke V, Pete J, Long DM, Gasser A, Tong DC, Arnstein M, Thorpe SR, Cooper ME, Forbes JM: Combination therapy with the advanced glycation end product cross-link breaker, alagebrium, and angiotensin converting enzyme inhibitors in diabetes: Synergy or redundancy? *Endocrinology* 148: 886–895, 2007
35. Bierhaus A, Haslbeck KM, Humpert PM, Liliensiek B, Dehmer T, Morcos M, Sayed AA, Andrassy M, Schiekofer S, Schneider JG, Schulz JB, Heuss D, Neundörfer B, Dierl S, Huber J, Tritschler H, Schmidt AM, Schwaninger M, Haering HU, Schleicher E, Kasper M, Stern DM, Arnold B, Nawroth PP: Loss of pain perception in diabetes is dependent on a receptor of the immunoglobulin superfamily. *J Clin Invest* 114: 1741–1751, 2004
36. Constien R, Forde A, Liliensiek B, Gröne HJ, Nawroth P, Hämmerling G, Arnold B: Characterization of a novel EGFP reporter mouse to monitor Cre recombination as demonstrated by a Tie2 Cre mouse line. *Genesis* 30: 36–44, 2001
37. Forbes JM, Yee LTL, Thallas V, Lassila M, Candido R, Jandeleit-Dahm K, Thomas MC, Burns WC, Deemer E, Thorpe SR, Cooper ME, Allen TJ: Advanced glycation end product interventions reduce diabetes accelerated atherosclerosis. *Diabetes* 53: 1813–1823, 2004
38. Vlassara H, Striker LJ, Teichberg S, Fuh H, Li YM, Steffes M: Advanced glycation end products induce glomerular sclerosis and albuminuria in normal rats. *Proc Natl Acad Sci U S A* 91: 11704–11708, 1994
39. Yonekura H, Yamamoto Y, Sakurai S, Petrova RG, Abedin MJ, Li H, Yasui K, Takeuchi M, Makita Z, Takasawa S, Okamoto H, Watanabe T, Yamamoto H: Novel splice variants of the receptor for advanced glycation end-products expressed in human vascular endothelial cells and pericytes, and their putative roles in diabetes-induced vascular injury. *Biochem J* 370: 1097–1109, 2003
40. Schulze-Lohoff E, Hugo C, Rost S, Arnold S, Gruber A, Brüne B, Sterzel RB: Extracellular ATP causes apoptosis and necrosis of cultured mesangial cells *via* P2Z/P2X7 receptors. *Am J Physiol* 275: F962–F971, 1998
41. Schlondorff D: Preparation and study of isolated glomeruli. *Methods Enzymol* 191: 130–140, 1990
42. Rahman S, Blok RB, Dahl HH, Danks DM, Kirby DM, Chow CW, Christodoulou J, Thorburn DR: Leigh syndrome: Clinical features and biochemical and DNA abnormalities. *Ann Neurol* 39: 343–351, 1996
43. Thorburn DR, Sugiana C, Salemi R, Kirby DM, Worgan L, Ohtake A, Ryan MT: Biochemical and molecular diagnosis of mitochondrial respiratory chain disorders. *Biochim Biophys Acta* 1659: 121–128, 2004
44. Nisselbaum JS, Green S: A simple ultramicro method for determination of pyridine nucleotides in tissues. *Anal Biochem* 27: 212–217, 1969

Supplemental information for this article is available online at http://www.jasn.org/.

Nephrol Dial Transplant (2009) 24: 1397–1406
doi: 10.1093/ndt/gfn659
Advance Access publication 28 November 2008

Original Articles

NDT
Nephrology Dialysis Transplantation

Administration of pigment epithelium-derived factor (PEDF) reduces proteinuria by suppressing decreased nephrin and increased VEGF expression in the glomeruli of adriamycin-injected rats

Toshiko Fujimura[1], Sho-ichi Yamagishi[2], Seiji Ueda[1], Kei Fukami[1], Ryo Shibata[1], Yuriko Matsumoto[1], Yusuke Kaida[1], Ayako Hayashida[1], Kiyomi Koike[1], Takanori Matsui[2], Kei-ichiro Nakamura[3] and Seiya Okuda[1]

[1]Division of Nephrology, Department of Medicine, [2]Department of Pathophysiology and Therapeutics of Diabetic Vascular Complications and [3]Division of Microscopic & Developmental Anatomy, Department of Anatomy, Kurume University School of Medicine, Kurume, Japan

Abstract

Background. Pigment epithelium-derived factor (PEDF) is a glycoprotein with potent neuronal differentiating activity. We, along with others, have recently found that PEDF inhibits retinal hyperpermeability by counteracting the biological effects of vascular endothelial growth factor (VEGF). However, the protective role of PEDF against nephrotic syndrome (NS), a condition of hyperpermeability in the glomerular capillaries, remains to be elucidated. In this study, we investigated whether and how PEDF reduced proteinuria in rats with adriamycin (ADR)-induced nephropathy (ADN), an experimental model of NS.

Methods. ADN was induced by a single intravenous injection of doxorubicin hydrochloride ($n = 12$). Half the ADN rats were intravenously administrated human recombinant PEDF; the other half were given vehicle everyday for up to 14 days. Control rats ($n = 6$) received vehicle only.

Results. In ADN, expression levels of PEDF in isolated glomeruli were significantly decreased, which were associated with a marked proteinuria and increased urinary excretion of nephrin, an index of podocyte damage. Loss of nephrin and decreased podocyte cell number and fusion of foot processes of podocytes with nuclear factor-kappa B (NF-κB) activation and VEGF overexpression were also observed in the glomeruli of rats with ADN. Intravenous administration of PEDF ameliorated all of these changes in ADN rats.

Conclusion. The present findings suggest that PEDF could reduce proteinuria by suppressing podocyte damage and decreased nephrin as well as increased VEGF expression in the glomeruli of ADN rats. Pharmacological up-regulation or substitution of PEDF may offer a promising therapeutic strategy for the treatment of nephrotic syndrome.

Keywords: hyperpermeability; nephrin; nephrotic syndrome; PEDF; VEGF

Introduction

Pigment epithelium-derived factor (PEDF) is a glycoprotein that belongs to the superfamily of serine protease inhibitors. It was first purified from the conditioned media of human retinal pigment epithelial cells as a factor that possesses potent neuronal differentiating activity in human retinoblastoma cells [1]. Recently, PEDF has been shown to be a highly effective inhibitor of angiogenesis in cell culture and animal models [2,3]. PEDF inhibits the growth and migration of cultured endothelial cells (ECs), and it potently suppresses ischaemia-induced retinal neovascularization [2,3]. Since PEDF levels in aqueous humour or vitreous fluid are decreased in diabetic patients, especially with proliferative retinopathy [4], the loss of PEDF activity in the eye may contribute to the development and progression of proliferative diabetic retinopathy.

In addition, we, along with others, have recently found that PEDF inhibits retinal hyperpermeability by counteracting the biological effects of vascular endothelial growth factor (VEGF) [5,6], thus suggesting that PEDF may be an important therapeutic adjunct in the treatment of a number of devastating disorders where increased vascular permeability is a pathological mechanism. PEDF is expressed in a broad range of human fetal and adult tissues including kidney [7–10]. Increases in vascular permeability in the kidney have been considered to play a key role in the development of nephrotic syndrome (NS) [11,12]. These findings led us to speculate that PEDF could exert beneficial effects on NS as well by suppressing the effects of VEGF. However, as

Correspondence and offprint requests to: Sho-ichi Yamagishi, Division of Cardiovascular Medicine, Department of Medicine, Kurume University School of Medicine, 67 Asahi-machi, Kurume 830-0011, Japan. Tel: +81-942-31-7580; Fax: +81-942-31-7707; E-mail: shoichi@med.kurume-u.ac.jp

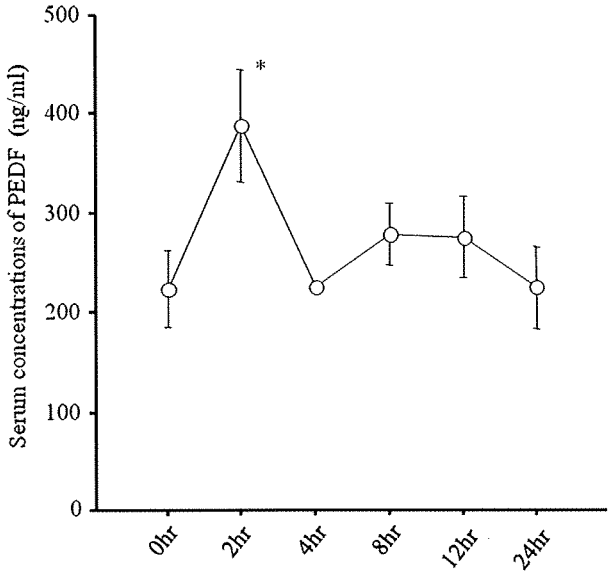

Fig. 1. Serum concentrations of PEDF in SD rats. SD 8-week-old rats were intravenously injected with 30 μg PEDF, and then the serum concentrations of PEDF were measured (each $n = 3$). $^*P < 0.05$ compared with the basal value at 0 h.

far as we know, the role of PEDF in NS remains to be elucidated. Therefore, we investigated here whether and how the administration of PEDF could reduce proteinuria in rats with adriamycin (ADR)-induced nephropathy (ADN), an experimental model of NS.

Subjects and methods

Experimental design

The experiments were performed on 8-week-old male Sprague-Dawley (SD) rats weighing ~300 g. ADN was induced in rats ($n = 12$) by a single intravenous injection of doxorubicin hydrochloride (6.0 mg/kg) diluted in 0.9% saline as previously described [13]. Half the ADN rats were intravenously administrated human recombinant PEDF (30 μg/body diluted in 0.9% saline); the other half were given vehicle everyday for up to 14 days. Control rats ($n = 6$) received vehicle only. We have previously shown that intravenous administration of 10–30 μg PEDF once a day exerted anti-thrombogenic, anti-permeability and anti-inflammatory effects in 9-week-old SD rats [6,14], whose body weights were nearly the same as those used in this experiment. This is a reason why we chose the treatment condition with intravenous administration of 30 μg PEDF once daily in our model. Rat body weights of each group were nearly equal (~300 g). Therefore, we injected 30 μg PEDF per rat, not per 300 g body weight in this experiment. We also confirmed here that the peak concentration of circulating PEDF level was obtained at 2 h after the 30 μg PEDF injection and its level was increased to about 2-fold of the basal level (Figure 1).

BP was measured by a tail-cuff sphygmomanometer using an automated system with a photoelectric sensor (BP-98A; Softron, Tokyo, Japan) on Days −1, 3, 7, 10 and 14. All of the rats were killed on Day 15 and the kidneys were excised for immunohistochemical, morphometric and western blot analysis. All experimental procedures were conducted in accord with the NIH Guide for *the Care and Use of Laboratory Animals* and were approved by the ethical committee of our institution.

Purification of the PEDF protein

The PEDF protein was prepared and purified as previously described [15]. SDS–PAGE analysis of the purified PEDF protein revealed a single band with a molecular mass of ~50 kDa, which showed positive reactivity with a monoclonal antibody against human PEDF (Transgenic, Kumamoto, Japan).

Measurements of clinical parameters

Plasma and urinary levels of total protein, plasma total cholesterol and albumin were determined with commercially available kits (Wako, Osaka, Japan). Plasma creatinine (Cr) levels were also measured with a commercial kit (Alfresa Pharma Co., Tokyo, Japan). Serum PEDF levels were measured with the ELISA as previously described [16].

Immunofluorescence staining

Frozen kidneys were embedded in a Tissue-Tek (Sakura Finetek, Torrance, CA, USA) 22-oxacalcitriol (OCT) medium and cut on a cryostat microtome into 4 μm sections. Tissue sections were fixed in 2% paraformaldehyde for 5 min at 4°C, and then blocked with 3% normal goat serum (Dako, Glostrup, Denmark). To determine the expression levels of PEDF in the kidney, we performed an indirect immunofluorescence staining with the rabbit anti-PEDF polyclonal antibody (Ab) (1:1000; BioProducts MD, Middletown, MD, USA) as a primary Ab. Further, the sections were double-stained with Abs raised against a podocyte marker, Wilm's tumour-1 (WT-1) (1:100; Dako Cytomation, Glostrup, Denmark), an EC marker, RECA-1 (1:200; AbD serotec, Raleigh, NC, USA) or a mesangial cell marker, Thy1.1 (1:100; Chemicon, Temecula, CA, USA). Goat anti-rabbit IgG Alexa 488 and anti-mouse IgG Alexa 594 (1:2000; Molecular Probes, Eugene, OR, USA) were used as secondary Abs. The samples were analysed under a confocal laser microscope, FV 1000 (OLYMPUS, Tokyo, Japan). Immunofluorescence staining of nephrin was performed using a rabbit polyclonal anti-nephrin Ab (Alpha Diagnostic, San Antonio, TX, USA) and evaluated with a semi-quantitative scoring system (0–4) according to the paper of Gross *et al.*: score 0, no expression; score 1, mild expression; score 2, moderate expression; score 3, strong expression; score 4, extremely strong expression [17]. All analyses were performed in a blinded manner, i.e. the observer was unaware of the experimental protocol.

Morphometric analysis

The kidneys were fixed in 4% paraformaldehyde and embedded in paraffin wax for sectioning. Three-micrometer

paraffin sections were stained with periodic acid-Schiff (PAS) for light microscopic analysis. For electron microscopic analysis, small blocks of the kidneys were fixed with 2.5% glutaraldehyde, post-fixed in 2% osmium tetroxide, dehydrated in graded ethanol, and then embedded in epoxy resin. The ultrathin section (0.1 μm) was stained with uranyl acetate and lead citrate.

Isolation of glomeruli

Glomeruli were isolated by the graded sieving method as previously described [18]. Briefly, rats were deeply anaesthetized and the kidneys were immediately removed. The cortex was excised, cut into fine fragments and homogenized. After being passed through consecutive stainless steel screens of 177-, 125- and 63-μm pore size, the glomeruli were suspended in phosphate-buffered saline and collected by centrifugation at 2000*g* for 3 min.

Western blot analysis of PEDF, VEGF and P50 subunit of nuclear factor-κB (NF-κB) and cAMP response element-binding protein (CREB)

Fifty micrograms of proteins extracted from isolated glomeruli, urine samples or cortical tissues was separated by SDS–PAGE and transferred to nitrocellulose membranes (Biorad, Hercules, CA, USA). Then, the membranes were blotted with anti-PEDF, anti-VEGF or anti-p50 subunit of NF-κB, and anti-CREB (Santa Cruz Biotechnology, Delaware, CA, USA) Abs. The immune complexes were visualized with an enhanced chemiluminescence detection system (ECL; Amersham Bioscience, Buckinghamshire, UK).

Preparation of nuclear extracts from kidney

Nuclear protein was extracted from cortical lesions of the kidney as previously described [19]. Briefly, 500 mg of cortical tissues was homogenized with 20 even strokes of a glass Teflon homogenizer in 1 mL of ice-cold buffer A [10 mM HEPES (pH 7.9), 10 mM KCl, 2 mM $MgCl_2$, 0.1 mM ethylenediaminetetraacetic acid (EDTA), and a cocktail of protease inhibitors (Nakarai Tesque, Kyoto, Japan)]. Then, 325 μL of detergent Nondiet-P40 (2%) was added. The mixture was vortexed 10 times for 1 min each and centrifuged at 13 000*g* for 5 min. The supernatant was removed, and then the pellet was re-suspended in 300 μL of buffer B [50 mM HEPES, 10% (v/v) glycerol, 300 mM NaCl, 50 mM KCl and the protease inhibitor cocktail]. The samples were centrifuged again and the supernatant (nuclear proteins) was stored in aliquots at −80°C. The protein concentrations were determined by a BCA protein assay kit (Pierce, Rockford, IL, USA).

Measurement of in situ reactive oxygen species (ROS) generation and urinary 8-isoprostane levels

The oxidative fluorescent probe dihydroethidium (DHE) (Invitrogen, Carlsbad, CA, USA) was used to detect *in situ* levels of ROS in the kidney as previously described [20]. Briefly, the tissue sections were embedded in an OCT medium and cut on a cryostat microtome into 4 μm sections. The sections were stained with 2 μM DHE for 30 min. *In situ* production of superoxide was visualized as a red fluorescence. We also measured urinary 8-isoprostane levels on Day 14 with an enzyme-linked immunoassay (8-iso-$PGF_{2\alpha}$ EIA kit; Oxford Biomedical Research, Oxford, MI, USA).

Statistical analysis

All data were expressed as mean ± SD. One-way ANOVA followed by the Scheffe *F*-test was performed for statistical comparisons. $P < 0.05$ was considered statistically significant.

Results

Immunofluorescence staining for PEDF-positive cells in normal rat kidney

PEDF is expressed in a broad range of human fetal and adult tissues including kidney [7–10]. Further, its levels are higher in renal cortex than those in the medulla [10,21]. However, the precise localization of PEDF-positive cells in the kidney remains to be determined. So, we first examined which types of cells were positive for PEDF staining in the kidney. PEDF was expressed in glomerular areas, arteries, veins and capillaries in normal rat kidneys (Figure 2A a). Negative control staining with 3% goat serum/PBS is shown in Figure 2A b. Double staining with anti-RECA-1 (Figure 2B a–d), anti-WT-1 (Figure 2B e–h) or anti-Thy1.1 Abs (Figure 2B i–l) revealed that PEDF was expressed in podocytes, ECs and mesangial cells. DAPI staining confirmed that PEDF was expressed within the cells (Figure 2C a, b).

PEDF expression levels in glomeruli of rats with ADN and PEDF-treated ADN

We next evaluated the expression levels of PEDF in the glomeruli with two different methods, immunofluorescence staining (Figure 3A) and western blot analysis (Figure 3B). As shown in Figure 3A, PEDF-positive immunofluorescence in the glomeruli of rats with ADN was significantly decreased, compared with that in control rats; the glomerular PEDF levels were reduced to ~4/5 of those of control rats (Figure 3B), which was prevented by the treatments with intravenous administration of PEDF (Figure 3A and B).

Effects of PEDF administration on proteinuria in ADN rats

In order to investigate the pathophysiological relevance of PEDF in ADN, we next examined the effects of PEDF on urinary protein excretion in ADN rats. As shown in Table 1, intravenous administration of PEDF significantly

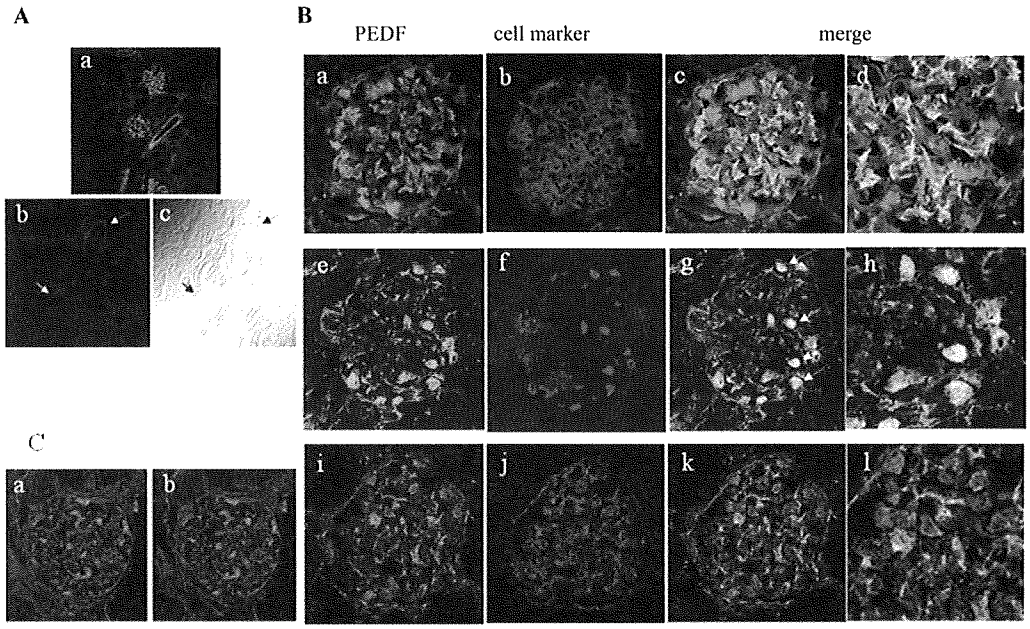

Fig. 2. Immunofluorescence staining for PEDF in kidney. (**A**) Immunofluorescence staining of PEDF. The sections were incubated with (a) or without (b) (negative staining) PEDF antibody (Ab). (c) is a phase contrast for (b). Magnification ×200. Arrow and arrowhead indicate the location of glomerulus and blood vessel, respectively. (**B**) Double staining of the glomeruli with PEDF Ab (a, e, i), anti-RECA-1 Ab (b), anti-WT-1 Ab (f) or anti-Thy1.1 Ab (j). PEDF-positive podocytes are indicated as arrows. Magnification: (a–c, e–g, i–k), ×400; (d, h, l), ×800. (**C**) PEDF immunofluoresscence with (a) or without (b) DAPI staining. Magnification ×600.

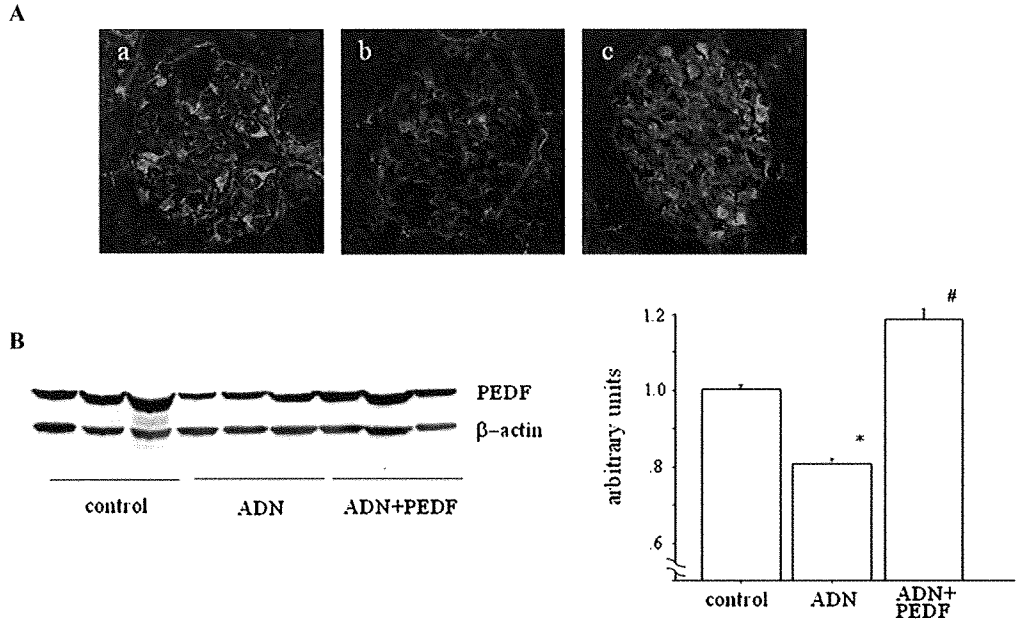

Fig. 3. PEDF expression in the glomeruli of control, ADN and PEDF-treated ADN rats. (**A**) Immunofluorescence staining for PEDF in control (a), ADN (b) and PEDF-treated ADN rats (c). Magnification ×600. (**B**) Western blot analysis of PEDF in the glomeruli isolated from control, ADN and PEDF-treated ADN rats. Left panel shows the representative results of western blots. Right panel shows the quantitative data. Data were normalized by the intensity of β-actin bands ($n = 6$, respectively). $^{*}P < 0.05$ compared with the controls, $^{\#}P < 0.05$ compared with the ADN rats.

reduced proteinuria and prevented the decrease in serum albumin as well as the increase in total cholesterol levels in ADN rats. Body weight and creatinine clearance (Ccr) were not different among three groups (Table 1). There was no significant difference in systolic blood pressure (SBP) among each group (Table 2).

Effects of PEDF administration on renal histopathology in ADN rats

Light microscopic examination showed subtle histopathological changes in glomerular and tubulointerstitial areas of the ADN rats (Figure 4). However, electron microscopic

Table 1. Clinical variables on Day 14

	BW (g)	UP (mg/day)	Alb (g/dL)	T.Chol (mg/dL)	Cr (mg/dL)	Ccr (mL/min)
Control rats	324 ± 11.6	19.3 ± 11.6	4.9 ± 0.23	58.7 ± 10.6	0.35 ± 0.03	2.8 ± 0.3
ADN rats	336 ± 12.9	344.1 ± 150.7[a]	3.0 ± 0.42[a]	188.8 ± 63.3[a]	0.29 ± 0.06[a]	3.1 ± 0.4
ADN rats + PEDF	344 ± 9.1	134.7 ± 67.8[b]	3.6 ± 0.28[a,b]	105.8 ± 20.4[b]	0.28 ± 0.01[a]	2.9 ± 0.4

BW, body weight; UP, urinary protein excretion; Alb, serum albumin; T.Chol, serum total cholesterol; Cr, serum creatinine; Ccr, 24-h creatinine clearance.
[a] $P < 0.05$ compared with control rats.
[b] $P < 0.05$ compared with ADN rats.

Table 2. Effects of PEDF administration on SBP in ADN rats

	Day 1	Day 3	Day 7	Day 10	Day 14
Control rats	117.0 ± 11.1	114.5 ± 15.7	115.7 ± 4.5	119.5 ± 6.6	115.5 ± 8.3
ADN rats	106.6 ± 10.5	123.9 ± 9.4	114.9 ± 15.1	118.2 ± 14.4	117.6 ± 5.8
ADN rats + PEDF	123.0 ± 8.5	113.6 ± 11.6	123.0 ± 7.7	113.0 ± 10.4	110.4 ± 7.2

SBP, systolic blood pressure (mmHg).

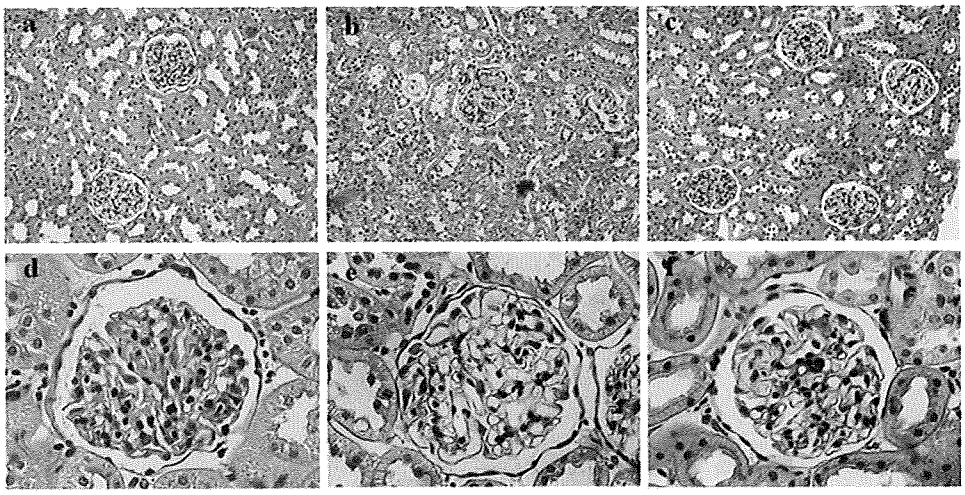

Fig. 4. Effects of PEDF administration on renal histopathology in ADN rats. Light microscopic examination showed subtle histopathological changes in glomerular and tubulointerstitial areas of the normal (**a**, **d**), ADN (**b**, **e**) and PEDF-treated ADN (**c**, **f**) rats. Magnification ×200 (a, b, c), ×600 (d, e, f)

examination revealed that foot processes of podocytes were fused in the ADN rats, which was significantly improved by the treatment of PEDF (Figure 5).

Effects of PEDF administration on podocyte loss and expression levels of nephrin in ADN rats

We next examined the number of podocyte and the expression levels of nephrin, which localizes to the slit pore of podocytes [22–24], in the glomeruli of ADN rats. Immunofluorescence staining revealed that the numbers of WT-1 positive (Figure 6A) or nephrin-positive cells (Figure 6B) were decreased in the glomeruli of ADN rats, compared with those of the control rats, both of which were partially restored by the treatment of PEDF.

Nephrin is excreted into urine in the early stages of experimental NS [24,25]. So, we next investigated whether PEDF administration reduced urinary excretion levels of nephrin in ADN rats. As shown in Figure 6C, nephrin was not detected in urine samples of the control rats. Urinary excretion levels of nephrin were increased in ADN rats, which were prevented by the treatment of PEDF.

Effects of PEDF administration on VEGF expression in the glomeruli of ADN rats

We next investigated the effects of PEDF administration on VEGF, a potent vasopermeability factor, expression in the glomeruli of ADN rats. VEGF expression was up-regulated in the glomeruli of ADN rats, which was significantly decreased by PEDF treatment (Figure 7).

Effects of PEDF on NF-κB activation in ADN rats

NF-κB is also known as one of the key mediators in experimental NS [19,26,27]. Therefore, in order to further investigate the molecular mechanism by which PEDF prevented the decrease in nephrin as well as the increase in VEGF

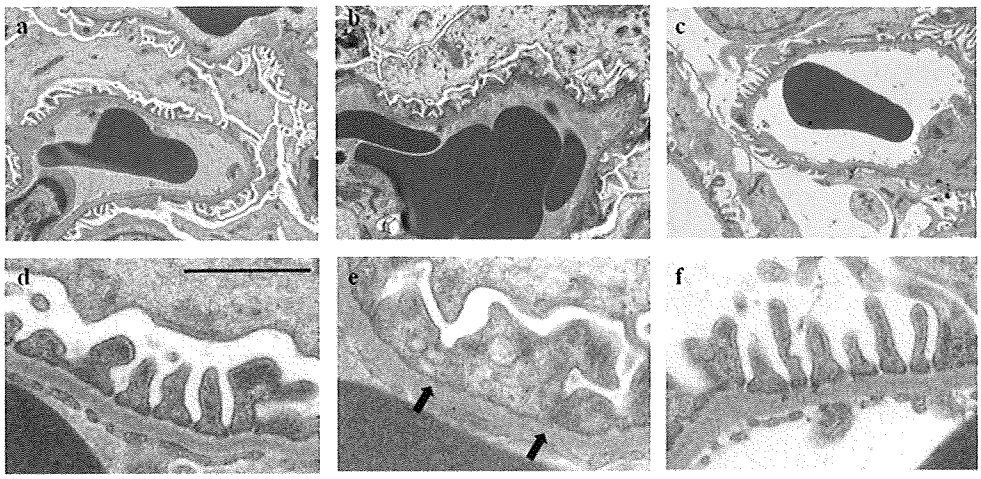

Fig. 5. Effects of PEDF administration on electron microscopic findings of the podocytes in ADN rats. Electron microscopic findings of the glomeruli in normal control (a, d), ADN (b, e) and PEDF-treated ADN rats (c, f). Magnification ×6000 (a–c), ×10 000 (d–f). The scale bar shows 0.5 μm. The arrows show the fusions of podocyte foot processes in ADN rats.

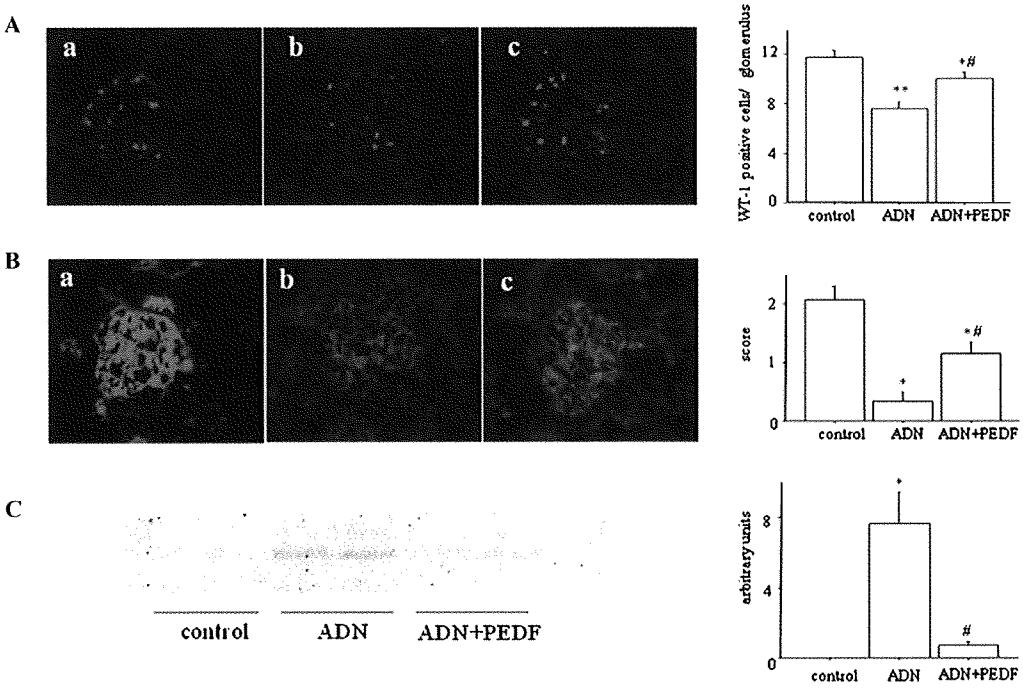

Fig. 6. Effects of PEDF administration on podocyte and expression levels of nephrin in ADN rats. (**A**) Immunofluorescence staining for WT-1, podocyte marker in normal control (a), ADN (b) and PEDF-treated ADN (c) rats. Right panel shows the number of WT-1 positive cells per glomerulus in these three groups ($n = 6$). $^{**}P < 0.0001$ compared with control, $^{*}P < 0.05$ compared with control, $^{\#}P < 0.05$ compared with ADN. (**B**) Immunofluorescence staining for nephrin in control (a), ADN (b) and PEDF-treated ADN rats (c). Magnification ×400. Right panel shows the glomerular nephrin staining scores ($n = 6$, respectively). $^{*}P < 0.05$ compared with the controls, $^{\#}P < 0.05$ compared with the ADN rats. (**C**) Effects of PEDF administration on urinary excretion levels of nephrin on ADN rats. Left panel shows the representative results of western blots. Right panel shows the quantitative data ($n = 6$, respectively). $^{*}P < 0.05$ compared with the controls, $^{\#}P < 0.05$ compared with the values of ADN rats.

expression in ADN rats, we investigated the effects of PEDF administration on NF-κB activation in the glomeruli of ADN rats. The p50 protein expression levels were densitometrically measured and normalized to the CREB expression because CREB is a nuclear marker protein [28]. As shown in Figure 8A, nucleus levels of p50 subunit of NF-κB were increased in the glomeruli of ADN rats, which were blocked by the treatment of PEDF. Since glyceraldehyde-3-phosphate dehydrogenase (GAPDH) is not a specific cytoplasmic marker protein and also exists in the nucleus [29], we were not able to confirm the purity of the nuclear extracts by western blots raised against GAPDH. We show a Comassie blue staining as a loading control in Figure 8B.

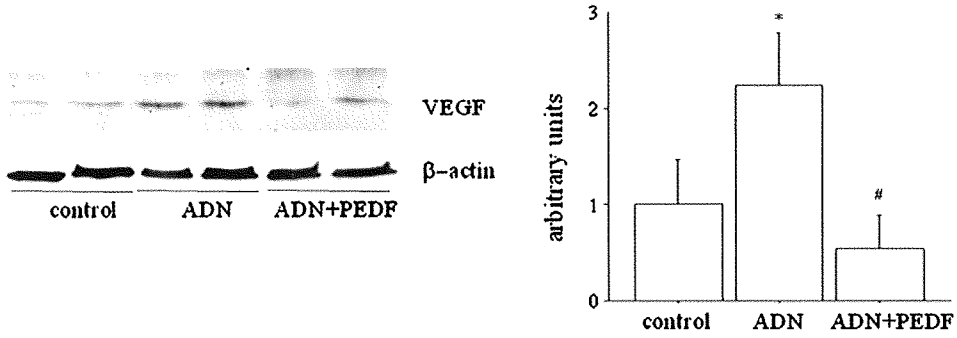

Fig. 7. Effects of PEDF administration on VEGF expression in the glomeruli of ADN rats. Left panel shows representative results of western blots. Right panel shows the quantitative data. Data were normalized by the intensity of β-actin bands ($n = 6$, respectively). $^{\#}P < 0.05$ compared with the values of ADN rats.

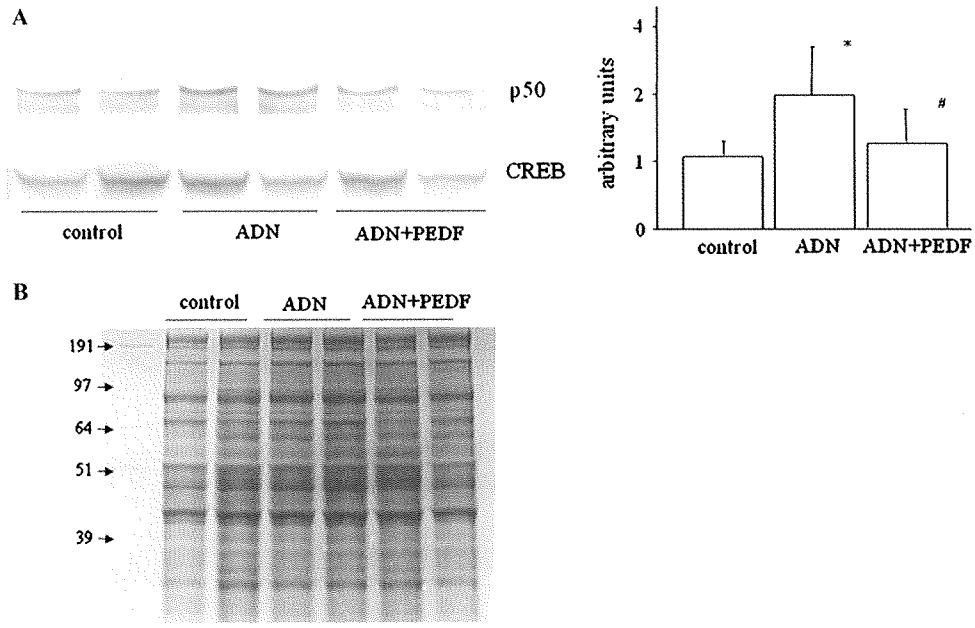

Fig. 8. Effects of PEDF administration on nuclear translocation of NF-κB p50 subunit in the glomeruli of ADN rats. (**A**) Left panel shows representative results of western blots of p50 and CREB. Right panel shows the quantitative data. The expression levels of p50 were normalized by the intensity of CREB bands ($n = 6$, respectively). $^{*}P < 0.05$ compared with the controls. $^{\#}P < 0.05$ compared with the values of ADN rats. (**B**) After electrophoresis, proteins were visualized with Coomassie blue staining.

Effects of PEDF administration on ROS generation in ADN rats

Since NF-κB is a redox-sensitive transcriptional factor [30], we further investigated the effects of PEDF on ROS generation in ADN rats. As shown in Figure 9, superoxide generation in the glomeruli and urinary excretion levels of oxidative stress marker, 8-isoprostane [31] were increased in ADN rats, both of which were not affected by the treatment of PEDF.

Discussion

We, along with others, have recently found that PEDF inhibits retinal hyperpermeability by counteracting the biological effects of VEGF [5,6], thus suggesting that PEDF may be a novel therapeutic strategy for the treatment of various disorders in which vasopermeability is involved. However, there are a few studies to show the implication of PEDF in the pathogenesis of proteinuria, a condition of barrier dysfunction of the glomerular capillary wall [21,32]. Indeed, Wang *et al.* only reported that PEDF levels were decreased in kidneys of streptozotocin-induced diabetic rats and that injection of adenovirus PEDF alleviated microalbuminuria and suppressed overexpression of two major fibrogenic factors, transforming growth factor-β and connective tissue growth factor in the diabetic kidneys [21,32]. In the present study, we have extended the previous findings that PEDF exerted salutary effects on proteinuria. We demonstrated here for the first time that administration of PEDF could reduce proteinuria by inhibiting podocytes loss as well as increased VEGF expression via blockade of NF-κB activation in the glomeruli of ADN rats, an experimental model of NS on the basis of the following evidence: (1) endogenous levels of glomerular PEDF expression levels

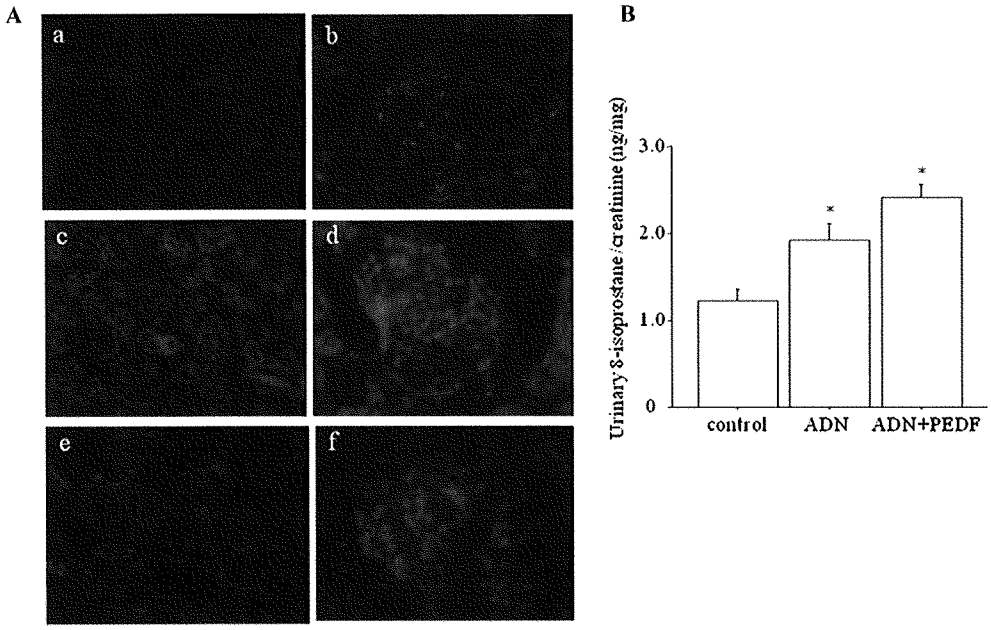

Fig. 9. Effect of PEDF administration on ROS generation in ADN rats. (**A**) Representative photographs of DHE staining of the glomeruli in control (a, b), ADN (c, d) and PEDF-treated ADN rats (e, f). Magnification ×100 in (a, c, e) and ×400 in (b, d, f). (**B**) Urinary excretion levels of 8-isoprostane/Cr. $^{*}P < 0.05$ compared with the controls.

were significantly decreased in ADN rats, compared with control rats; (2) administration of PEDF to ADN rats significantly ameliorated the decrease in glomerular PEDF levels and subsequently reduced proteinuria and prevented fusion of foot processes of podocytes and loss of podocytes in the glomeruli; (3) PEDF treatment also decreased urinary excretion levels of nephrin, an index of podocyte damage in ADN rats; and (4) NF-κB activation and VEGF up-regulation in the glomeruli of ADN rats were significantly blocked by the treatment of PEDF.

Nephrin is a key component of the slit diaphragm, the main site of control of glomerular permeability [22–24]. Indeed, nephrin mRNA or protein levels were reported to decrease in the glomeruli of various experimental models of hypertension, diabetes and membranous nephropathy, thereby being involved in proteinuria in these models [24,33–36]. In addition, nephrin is excreted into urine in the early stages of experimental NS and human diabetic nephropathy [24,25,35,36]. These observations suggest that the loss of nephrin may play a role in the pathogenesis of NS and urinary nephrin excretion could be a biomarker of podocyte damage in NS [24,25]. In the present study, we found that PEDF administration ameliorated loss of podocyte and nephrin in the glomeruli as well as the increase in its urinary excretion in ADN rats. Further, loss of podocytes and fusion of podocyte foot processes in ADN rats were prevented by the treatment of PEDF. Taken together, the present findings suggest that PEDF may have a protective role against podocyte damage and subsequently reduce proteinuria in ADN rats.

VEGF is expressed in foot processes of podocytes [37,38]. There is a growing body of evidence that podocyte-derived VEGF may play a central role in the maintenance of glomerular capillary permeability as well as the regulation of proteinuria in various types of NS [39–42]. In this study, VEGF expression was up-regulated in the glomeruli of ADN rats, which was prevented by the treatment of PEDF. These observations suggest that VEGF-elicited vascular permeability in the kidney may be counterbalanced by glomerular PEDF and that PEDF administration could ameliorate proteinuria, by not only restoring the loss of podocytes and decreased nephrin expression but also suppressing VEGF levels in the glomeruli of ADN rats. Since VEGF is a potent vasodilator, it would be possible that the inhibition of VEGF (the proposed mechanism of PEDF) may reduce tissue perfusion, flow and area, thereby decreasing proteinuria in ADN rats [43]. However, as we have reported in the previous paper [6], PEDF significantly inhibits the decrease in transendothelial electrical resistance, an indicator of EC barrier function in advanced glycation end-product-exposed ECs, by suppressing VEGF expression. Therefore, PEDF could improve barrier function in ECs, independent of vessel area or flow. Furthermore, we found here that PEDF treatment did not affect systemic blood pressure (Table 2) or Ccr in ADN rats (Table 1). These findings suggest that PEDF treatment may mainly decrease proteinuria in ADN rats through its anti-permeability effect, but not its haemodynamic one, via suppression of VEGF.

In this study, we found that expression levels of NF-κB p50 subunit in nuclei of the glomeruli were increased in ADN rats, which was blocked by the treatment of PEDF. Suppression of the NF-κB activation may be a central mechanism by which PEDF inhibited the ADR-induced decrease in podocyte number and nephrin expression as well as the increase in VEGF generation in the glomeruli on the basis of the following evidence: (1) NF-κB activation was associated with the loss of nephrin expression and proteinuria in anti-glomerular basement membrane nephritis [27];

(2) podocyte NF-κB overactivation was observed in patients with non-proliferative glomerulopathy and its levels were positively correlated with the severity of proteinuria in those patients [44] and (3) NF-κB binding site exists in the promoter region of VEGF and that NF-κB activation is indispensable for VEGF gene induction in various types of disorders [45–47]. Although we did not know the molecular mechanisms underlying the ADR-induced NF-κB activation, PEDF may suppress the NF-κB activation in the glomeruli of ADN rats in an ROS-independent manner because we found here that PEDF did not affect ROS generation in ADN rats by two distinct methods: one is DHE staining that can detect *in situ* superoxide production, and the other is the measurement of urinary 8-isoprostane excretion.

There are some limitations of the present study. Due to technical reasons, we were not able to study the potential benefit of a more continuous administration of PEDF in ADN and to include an additional group of PEDF-treated healthy rats. However, we already confirmed in another study (unpublished data) that intravenous PEDF administration to normal rats for 2 weeks increased serum PEDF levels to 150 ng/mL, which had no effect on urinary albumin excretion levels (control rats versus PEDF-injected rats; 0.03 ± 0.01 versus 0.04 ± 0.02 mg albumin/g creatinine).

In conclusion, our present study suggests that pharmacological up-regulation or substitution of PEDF may offer a promising therapeutic strategy for the treatment of NS.

Acknowledgements. This work was supported in part by Grants of Venture Research and Development Centers from the Ministry of Education, Culture, Sports, Science and Technology, Japan, to S.Y.

Conflict of interest statement. None declared.

References

1. Tombran-Tink J, Chader GG, Johnson LV. PEDF, a pigment epithelium-derived factor with potent neuronal differentiative activity. *Exp Eye Res* 1991; 53: 411–414
2. Mori K, Duh E, Gehlbach P *et al.* Pigment epithelium-derived factor inhibits retinal and choroidal neovascularization. *J Cell Physiol* 2001; 188: 253–263
3. Stellmach V, Crawford SE, Zhou W *et al.* Prevention of ischemia-induced retinopathy by the natural ocular antiangiogenic agent pigment epithelium-derived factor. *Proc Natl Acad Sci USA* 2001; 98: 2593–2597
4. Spranger J, Osterhoff M, Reimann M *et al.* Loss of the antiangiogenic pigment epithelium-derived factor in patients with angiogenic eye disease. *Diabetes* 2001; 50: 2641–2645
5. Liu H, Ren JG, Cooper WL *et al.* Identification of the antivasopermeability effect of pigment epithelium-derived factor and its active site. *Proc Natl Acad Sci U S A* 2004; 101: 6605–6610
6. Yamagishi S, Nakamura K, Matsui T *et al.* Pigment epithelium-derived factor inhibits advanced glycation end product-induced retinal vascular hyperpermeability by blocking reactive oxygen species-mediated vascular endothelial growth factor expression. *J Biol Chem* 2006; 281: 20213–20220
7. Tombran-Tink J, Barnstable CJ. PEDF: a multifaceted neurotrophic factor. *Nat Rev Neurosci* 2003; 4: 628–636
8. Tombran-Tink J, Barnstable CJ. Therapeutic prospects for PEDF: more than a promising angiogenesis inhibitor. *Trends Mol Med* 2003; 9: 244–250
9. Karakousis PC, John SK, Behling KC *et al.* Localization of pigment epithelium derived factor (PEDF) in developing and adult human ocular tissues. *Mol Vis* 2001; 7: 154–163
10. Tombran-Tink J, Mazuruk K, Rodriguez IR *et al.* Organization, evolutionary conservation, expression and unusual Alu density of the human gene for pigment epithelium-derived factor, a unique neurotrophic serpin. *Mol Vis* 1996; 2: 11
11. Shulman K, Rosen S, Tognazzi K *et al.* Expression of vascular permeability factor (VPF/VEGF) is altered in many glomerular diseases. *J Am Soc Nephrol* 1996; 7: 661–666
12. Brenchley PE. Vascular permeability factors in steroid-sensitive nephrotic syndrome and focal segmental glomerulosclerosis. *Nephrol Dial Transplant* 2003; 18: vi21–vi25
13. Rangan GK, Pippin JW, Couser WG. C5b-9 regulates peritubular myofibroblast accumulation in experimental focal segmental glomerulosclerosis. *Kidney Int* 2004; 66: 1838–1848
14. Takenaka K, Yamagishi SI, Matsui T *et al.* Pigment epithelium-derived factor (PEDF) administration inhibits occlusive thrombus formation in rats: a possible participation of reduced intraplatelet PEDF in thrombosis of acute coronary syndromes. *Atherosclerosis* 2008; 197: 25–33
15. Yamagishi S, Inagaki Y, Amano S *et al.* Pigment epithelium-derived factor protects cultured retinal pericytes from advanced glycation end product-induced injury through its antioxidative properties. *Biochem Biophys Res Commun* 2002; 296: 877–882
16. Yamagishi S, Adachi H, Abe A *et al.* Elevated serum levels of pigment epithelium-derived factor in the metabolic syndrome. *J Clin Endocrinol Metab* 2006; 91: 2447–2450
17. Gross ML, El-Shakmak A, Szabo A *et al.* ACE-inhibitors but not endothelin receptor blockers prevent podocyte loss in early diabetic nephropathy. *Diabetologia* 2003; 46: 856–868
18. Fukami K, Ueda S, Yamagishi S *et al.* AGEs activate mesangial TGF-beta-Smad signaling via an angiotensin II type I receptor interaction. *Kidney Int* 2004; 66: 2137–2147
19. Rangan GK, Wang Y, Tay YC *et al.* Inhibition of nuclear factor-kappaB activation reduces cortical tubulointerstitial injury in proteinuric rats. *Kidney Int* 1999; 56: 118–134
20. Yamagishi S, Abe R, Inagaki Y *et al.* Minodronate, a newly developed nitrogen-containing bisphosphonate, suppresses melanoma growth and improves survival in nude mice by blocking vascular endothelial growth factor signaling. *Am J Pathol* 2004; 165: 1865–1874
21. Wang JJ, Zhang SX, Lu K *et al.* Decreased expression of pigment epithelium-derived factor is involved in the pathogenesis of diabetic nephropathy. *Diabetes* 2005; 54: 243–250
22. Hudson BG, Kalluri R, Gunwar S *et al.* Structure and organization of type IV collagen of renal glomerular basement membrane. *Contrib Nephrol* 1994; 107: 163–167
23. Ruotsalainen V, Patrakka J, Tissari P *et al.* Role of nephrin in cell junction formation in human nephrogenesis. *Am J Pathol* 2000; 157: 1905–1916
24. Nakatsue T, Koike H, Han GD *et al.* Nephrin and podocin dissociate at the onset of proteinuria in experimental membranous nephropathy. *Kidney Int* 2005; 67: 2239–2253
25. Patari A, Forsblom C, Havana M *et al.* Nephrinuria in diabetic nephropathy of type 1 diabetes. *Diabetes* 2003; 52: 2969–2974
26. Josko J, Mazurek M. Transcription factors having impact on vascular endothelial growth factor (VEGF) gene expression in angiogenesis. *Med Sci Monit* 2004; 10: RA89–RA98
27. Peltier J, Bellocq A, Perez J *et al.* Calpain activation and secretion promote glomerular injury in experimental glomerulonephritis: evidence from calpastatin-transgenic mice. *J Am Soc Nephrol* 2006; 17: 3415–3423
28. Chrivia JC, Kwok RP, Lamb N *et al.* Phosphorylated CREB binds specifically to the nuclear protein CBP. *Nature* 1993; 365: 855–859
29. Kodama R, Kondo T, Yokote H *et al.* Nuclear localization of glyceraldehyde-3-phosphate dehydrogenase is not involved in the initiation of apoptosis induced by 1-methyl-4-phenyl-pyridium iodide (MPP+). *Genes Cells* 2005; 10: 1211–1219
30. Li Q, Engelhardt JF. Interleukin-1beta induction of NFkappaB is partially regulated by H_2O_2-mediated activation of NFkappaB-inducing kinase. *J Biol Chem* 2006; 281: 1495–1505

31. Roberts LJ, Morrow JD. Measurement of F(2)-isoprostanes as an index of oxidative stress *in vivo*. *Free Radic Biol Med* 2000; 28: 505–513
32. Wang JJ, Zhang SX, Mott R *et al.* Salutary effect of pigment epithelium-derived factor in diabetic nephropathy: evidence for antifibrogenic activities. *Diabetes* 2006; 55: 1678–1685
33. Bonnet F, Cooper ME, Kawachi H *et al.* Irbesartan normalises the deficiency in glomerular nephrin expression in a model of diabetes and hypertension. *Diabetologia* 2001; 44: 874–877
34. Forbes JM, Bonnet F, Russo LM *et al.* Modulation of nephrin in the diabetic kidney: association with systemic hypertension and increasing albuminuria. *J Hypertens* 2002; 20: 985–992
35. Yuan H, Takeuchi E, Taylor GA *et al.* Nephrin dissociates from actin, and its expression is reduced in early experimental membranous nephropathy. *J Am Soc Nephrol* 2002; 13: 946–956
36. Cohen MP, Chen S, Ziyadeh FN *et al.* Evidence linking glycated albumin to altered glomerular nephrin and VEGF expression, proteinuria, and diabetic nephropathy. *Kidney Int* 2005; 68: 1554–1561
37. Brown LF, Berse B, Tognazzi K *et al.* Vascular permeability factor mRNA and protein expression in human kidney. *Kidney Int* 1992; 42: 1457–1461
38. Monacci WT, Merrill MJ, Oldfield EH. Expression of vascular permeability factor/vascular endothelial growth factor in normal rat tissues. *Am J Physiol* 1993; 264: C995–C1002
39. Kanellis J, Levidiotis V, Khong T *et al.* A study of VEGF and its receptors in two rat models of proteinuria. *Nephron Physiol* 2004; 96: 26–36
40. Bailey E, Bottomley MJ, Westwell S *et al.* Vascular endothelial growth factor mRNA expression in minimal change, membranous, and diabetic nephropathy demonstrated by non-isotopic *in situ* hybridisation. *J Clin Pathol* 1999; 52: 735–738
41. Wendt TM, Tanji N, Guo J *et al.* RAGE drives the development of glomerulosclerosis and implicates podocyte activation in the pathogenesis of diabetic nephropathy. *Am J Pathol* 2003; 162: 1123–1137
42. Eremina V, Sood M, Haigh J *et al.* Glomerular-specific alterations of VEGF-A expression lead to distinct congenital and acquired renal diseases. *J Clin Invest* 2003; 111: 707–716
43. Webb NJ, Watson CJ, Roberts IS *et al.* Circulating vascular endothelial growth factor is not increased during relapses of steroid-sensitive nephrotic syndrome. *Kidney Int* 1999; 55: 1063–1071
44. Zheng L, Sinniah R, Hsu SI. *In situ* glomerular expression of activated NF-kappaB in human lupus nephritis and other non-proliferative proteinuric glomerulopathy. *Virchows Arch* 2006; 448: 172–183
45. Bian ZM, Elner SG, Elner VM. Regulation of VEGF mRNA expression and protein secretion by TGF-beta2 in human retinal pigment epithelial cells. *Exp Eye Res* 2007; 84: 812–822
46. Suh J, Rabson AB. NF-kappaB activation in human prostate cancer: important mediator or epiphenomenon? *J Cell Biochem* 2004; 91: 100–117
47. Coughlan MT, Thallas-Bonke V, Pete J *et al.* Combination therapy with the advanced glycation end product cross-link breaker, alagebrium, and angiotensin converting enzyme inhibitors in diabetes: synergy or redundancy? *Endocrinology* 2007; 148: 886–895

Received for publication: 7.2.08
Accepted in revised form: 3.11.08

Nephrol Dial Transplant (2009) 24: 1406–1416
doi: 10.1093/ndt/gfn662
Advance Access publication 4 December 2008

BMP-7 fails to attenuate TGF-β1-induced epithelial-to-mesenchymal transition in human proximal tubule epithelial cells

Paul L. Dudas, Rochelle L. Argentieri and Francis X. Farrell

Department of Immunology Research, Centocor Research and Development, Inc., Radnor, PA 19087, USA

Abstract

Background. In rodent models of chronic renal disease bone morphogenetic protein-7 (BMP-7) has been shown to halt disease progression and promote recovery. Subsequent studies utilizing immortalized rodent renal cell lines showed that BMP-7 was renoprotective by antagonizing TGF-β1-stimulated epithelial-to-mesenchymal transition (EMT). The present study sought to determine if BMP-7 prevents TGF-β1-induced EMT in primary (RPTEC) and immortalized (HK-2) human proximal tubule epithelial cells.

Methods. EMT was determined by quantitative real-time PCR analysis of e-cadherin, vimentin, CTGF and TGF-β1 transcript expression and immunocytochemical analysis of ZO-1 and α-smooth muscle actin (α-SMA) protein expression following TGF-β1 treatment in RPTEC and HK-2 cells.

Results. In RPTEC and HK-2 cells, TGF-β1 significantly reduced e-cadherin expression and significantly increased vimentin, CTGF and TGF-β1 expression. TGF-β1 also diminished ZO-1 immunoreactivity and increased α-SMA expression in confluent cell monolayers. Co-incubation of TGF-β1 with an anti-TGF-β1 neutralizing antibody substantially reduced the cytokine's effects, which indicated EMT in these cells was inhibitable. Co-administration of BMP-7 over a broad concentration range (0.01–100 μg/ml) with TGF-β1 failed to attenuate EMT in RPTEC or HK-2

Correspondence and offprint requests to: Paul L. Dudas, Department of Immunology Research, Centocor Research and Development, Inc., 145 King of Prussia Road, R-4-2, Radnor, PA 19087, USA. Tel: +1-610-240-5595; Fax: +1-610-889-4418; E-mail: pdudas@its.jnj.com